Dark Matter Axions

Pierre Sikivie

17th International Workshop on Neutrino Telescopes

Venice, March 15, 2017

Outline

- Axion motivation and properties
- Production in the early universe and Bose-Einstein condensation
- Axion search methods

The Strong CP Problem

$$\mathcal{L}_{\mathrm{QCD}} = \ \ldots \ + \ \bar{\theta} \frac{g^2}{32\pi^2} G^a_{\mu\nu} \tilde{G}^{a\mu\nu}$$

where

$$\bar{\theta} = \theta - \arg\left(m_u \, m_d \ \ldots \ m_t\right)$$
$$= \theta - \arg\det\left(Y^u \, Y^d\right)$$

The absence of P and CP violation in the strong interactions requires

$$\bar{\theta} \leq 10^{-10}$$

from upper limit
on the neutron electric
dipole moment

If a $\mathrm{U}_{\mathrm{PQ}}(1)$ symmetry is assumed,

$$\mathcal{L} = \ldots + \frac{a}{f_a}\frac{g^2}{32\pi^2}G^a_{\mu\nu}\tilde{G}^{a\mu\nu} + \frac{1}{2}\partial_\mu a \partial^\mu a$$

$\bar{\theta} = \dfrac{a}{f_a}$ relaxes to zero,

and a light neutral pseudoscalar particle is predicted: the axion.

Weinberg, Wilczek 1978

$$m_a \simeq 6 \text{ eV} \frac{10^6 \text{ GeV}}{f_a}$$

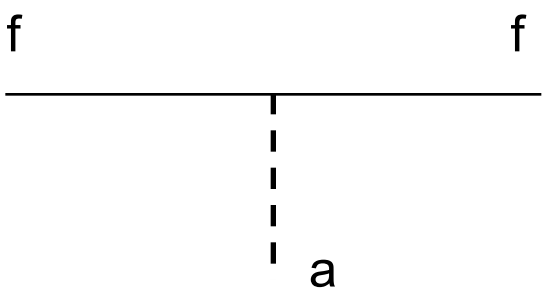

$$\mathcal{L}_{a\bar{f}f} = i g_f \frac{a}{f_a} \bar{f} \gamma_5 f$$

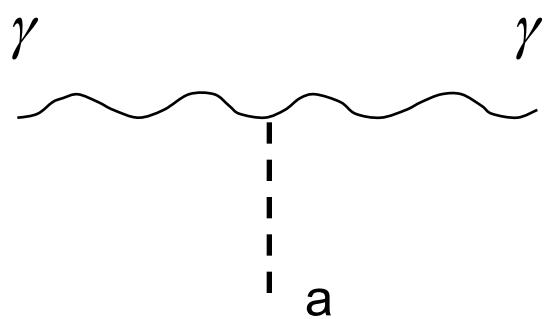

$$\mathcal{L}_{a\gamma\gamma} = g_\gamma \frac{a}{f_a} \vec{E} \cdot \vec{B}$$

g_γ = 0.97 in KSVZ model
0.36 in DFSZ model

The remaining axion window

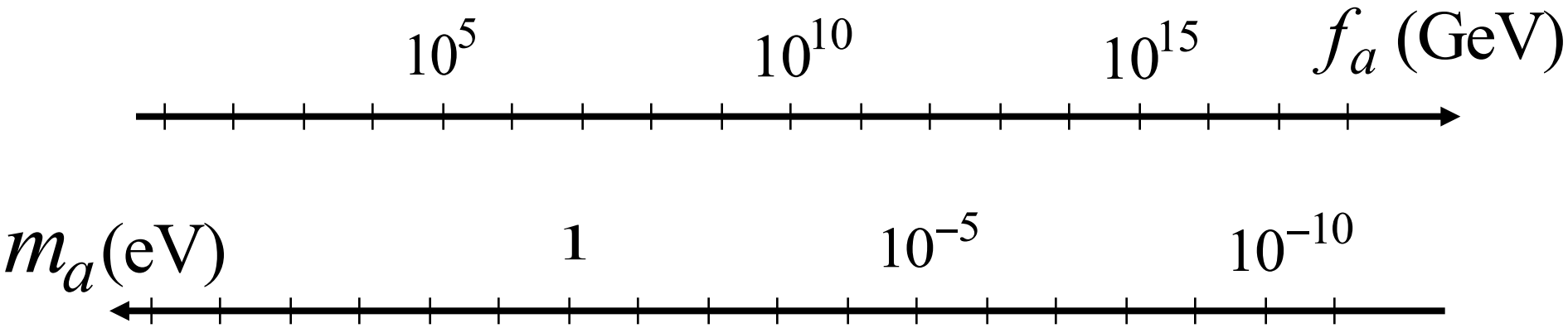

laboratory searches

cosmology

stellar evolution

Axion production by vacuum realignment

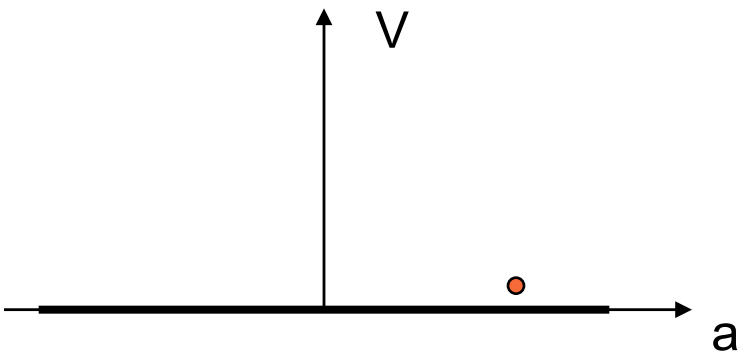

$T \geq 1\,\mathrm{GeV}$

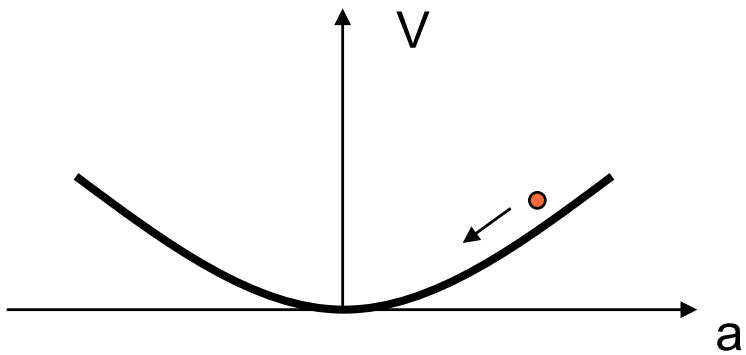

$T \leq 1\,\mathrm{GeV}$

$$n_a(t_1) \simeq \frac{1}{2} m_a(t_1) a(t_1)^2 \simeq \frac{1}{2t_1} f_a^2 \alpha(t_1)^2$$

$$\rho_a(t_0) \simeq m_a n_a(t_1) \left(\frac{R_1}{R_0}\right)^3 \propto m_a^{-\frac{7}{6}}$$

initial misalignment angle

J. Preskill, M. Wise & F. Wilczek, L. Abbott & PS, M. Dine & W. Fischler, 1983

Axions are cold dark matter

Density

$$\Omega_a \sim \left(\frac{10^{-5}\ \mathrm{eV}}{m_a}\right)^{\frac{7}{6}} \alpha(t_1)^2$$

Velocity dispersion

$$\delta v_a(t_0) \sim 3 \cdot 10^{-17} c \left(\frac{10^{-5}\ \mathrm{eV}}{m_a}\right)^{\frac{5}{6}}$$

Phase space density

$$\mathcal{N} = \frac{(2\pi)^3 n(t)}{\frac{4\pi}{3}(m_a \delta v)^3} \simeq 10^{61} \left(\frac{f_a}{10^{12}\ \mathrm{GeV}}\right)^{\frac{8}{3}}$$

Bose-Einstein Condensation

if identical bosonic particles
are highly condensed in phase space
and their total number is conserved
and they thermalize

then most of them go to the lowest energy
available state

why do they do that?

by yielding their energy to the non-condensed particles, the total entropy is increased.

preBEC

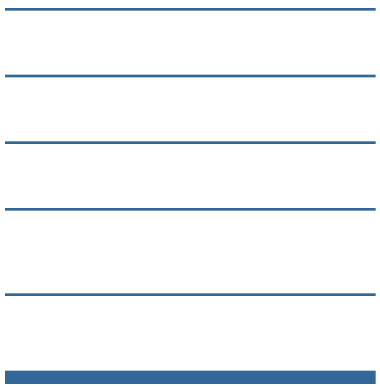

BEC

the axions thermalize and form a BEC after a time τ

$t < \tau$

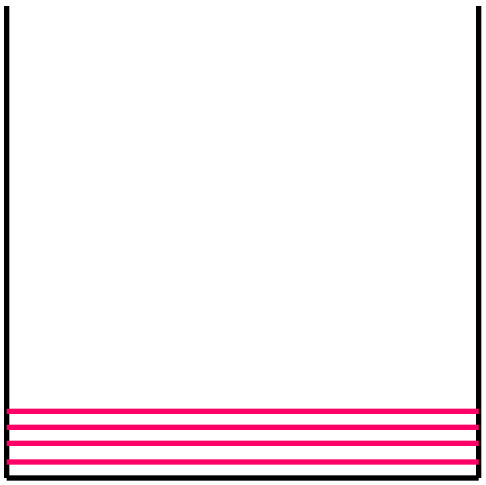

the axion fluid obeys classical field equations, behaves like CDM

$t > \tau$

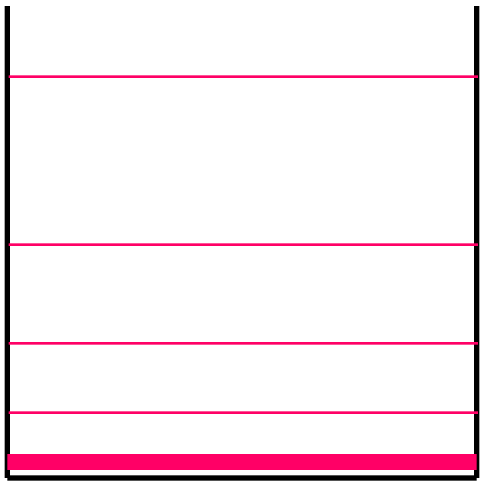

the axion fluid does not obey classical field equations, does not behave like CDM

the axion BEC rethermalizes

$t < \tau$

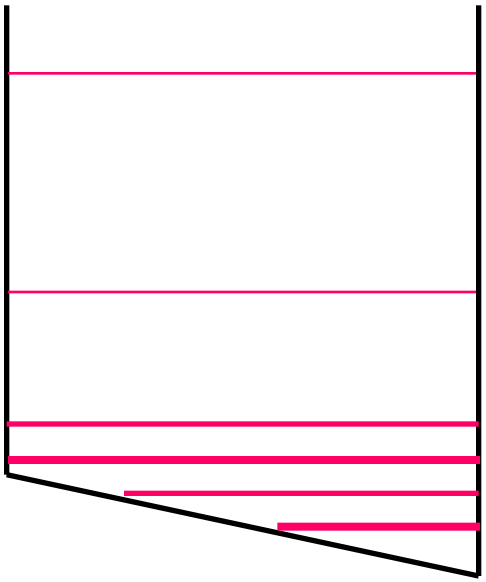

the axion fluid obeys
classical field equations,
behaves like CDM

$t > \tau$

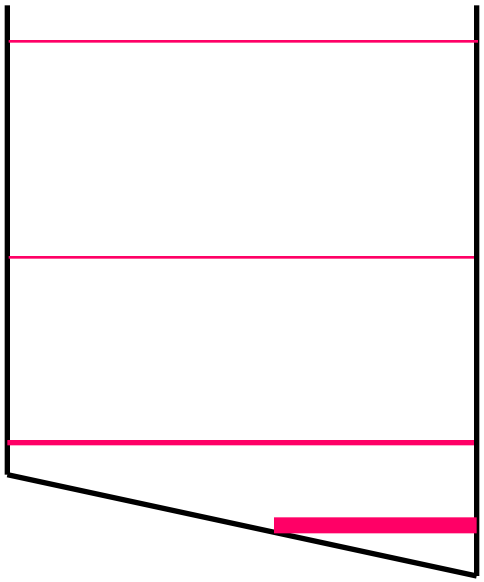

the axion fluid does not obey
classical field equations,
does not behave like CDM

$$\tau = ?$$

Quantum axion field dynamics

$$H = \sum_j \omega_j a_j^\dagger a_j \quad + \quad \sum_{ijkl} \frac{1}{4} \Lambda_{kl}^{ij} a_k^\dagger a_l^\dagger a_i a_j$$

O. Erken et al., PRD 85 (2012) 063520

From $\frac{1}{4!}\lambda\phi^4$ self-interactions

$$\Lambda_\lambda{}^{\vec{p}_3,\vec{p}_4}_{\vec{p}_1,\vec{p}_2} = -\frac{\lambda}{4m^2V}\,\delta_{\vec{p}_1+\vec{p}_2,\vec{p}_3+\vec{p}_4}$$

From gravitational self-interactions

$$\Lambda_g{}^{\vec{p}_3,\vec{p}_4}_{\vec{p}_1,\vec{p}_2} = -\frac{4\pi G m^2}{V}\,\delta_{\vec{p}_1+\vec{p}_2,\vec{p}_3+\vec{p}_4}\left(\frac{1}{|\vec{p}_1-\vec{p}_3|^2}+\frac{1}{|\vec{p}_1-\vec{p}_4|^2}\right)$$

Thermalization occurs due to gravitational interactions

PS + Q. Yang, PRL 103 (2009) 111301

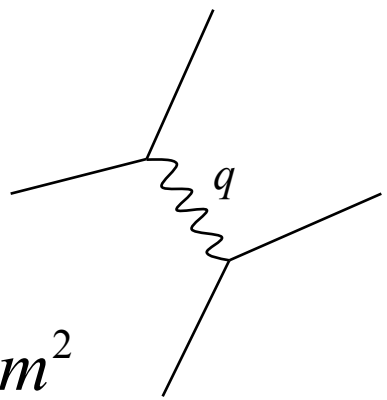

$$\frac{Gm^2}{q^2}$$

$$\Gamma_g \sim 4\pi G n m^2 l^2 \qquad \text{with } l = (m\,\delta \mathrm{v})^{-1}$$

$$\sim 5 \cdot 10^{-7} H(t_1) \left(\frac{f}{10^{12}\ \mathrm{GeV}} \right)^{\frac{2}{3}}$$

at time t_1

$$\Gamma_g(t)/H(t) \propto t\, a(t)^{-1} \propto a(t)$$

Gravitational interactions thermalize the axions and cause them to form a BEC when the photon temperature

$$T_\gamma \sim 500 \text{ eV} \left(\frac{f}{10^{12} \text{ GeV}} \right)^{\frac{1}{2}}$$

After that

$$\delta v \sim \frac{1}{mt}$$

$$\Gamma_g(t) / H(t) \propto t^3 \, a(t)^{-3}$$

Tidal torque theory

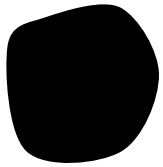

neighboring
protogalaxy

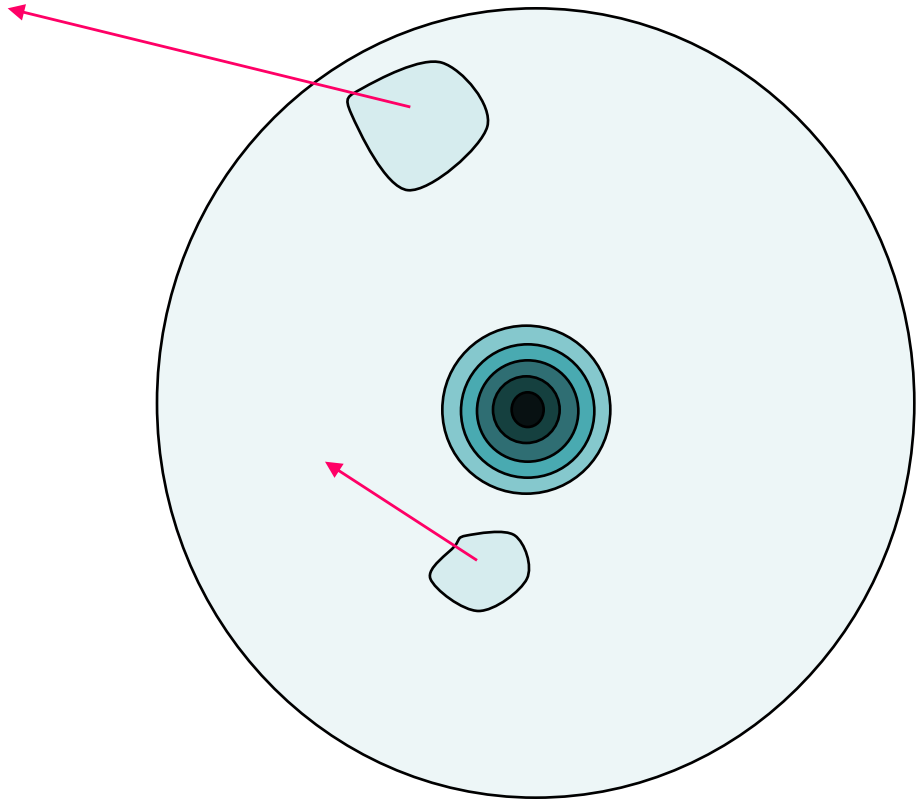

Stromberg 1934; Hoyle 1947; Peebles 1969, 1971

Tidal torque theory with ordinary CDM

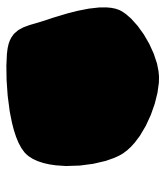

neighboring protogalaxy

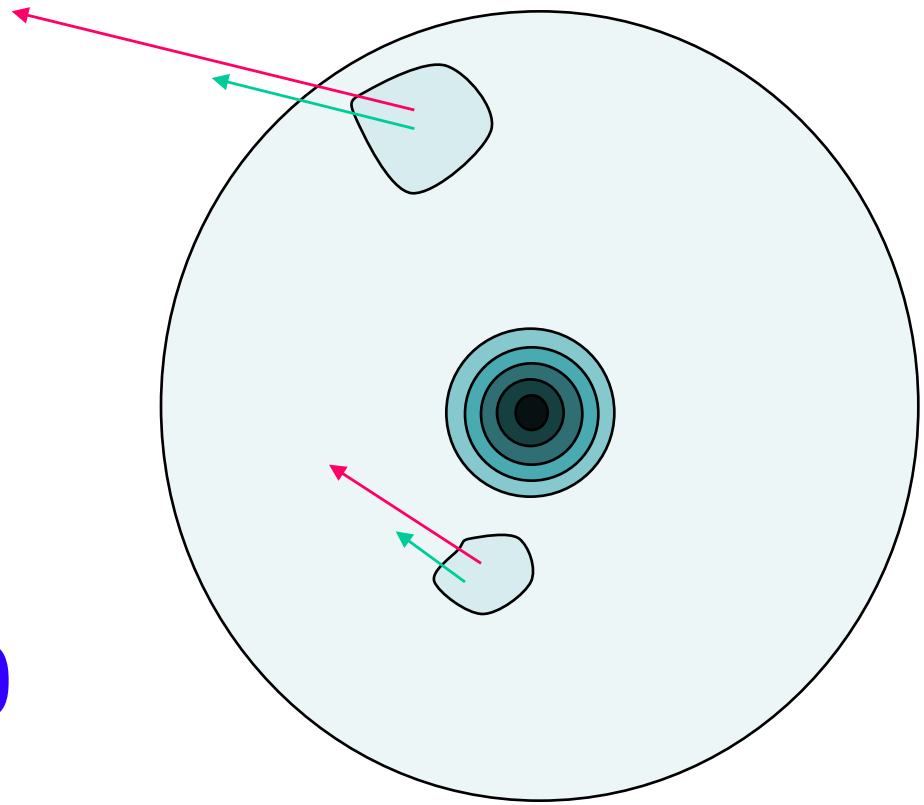

$$\vec{\nabla} \times \vec{v} = 0$$

the velocity field remains irrotational

Tidal torque theory with axion BEC

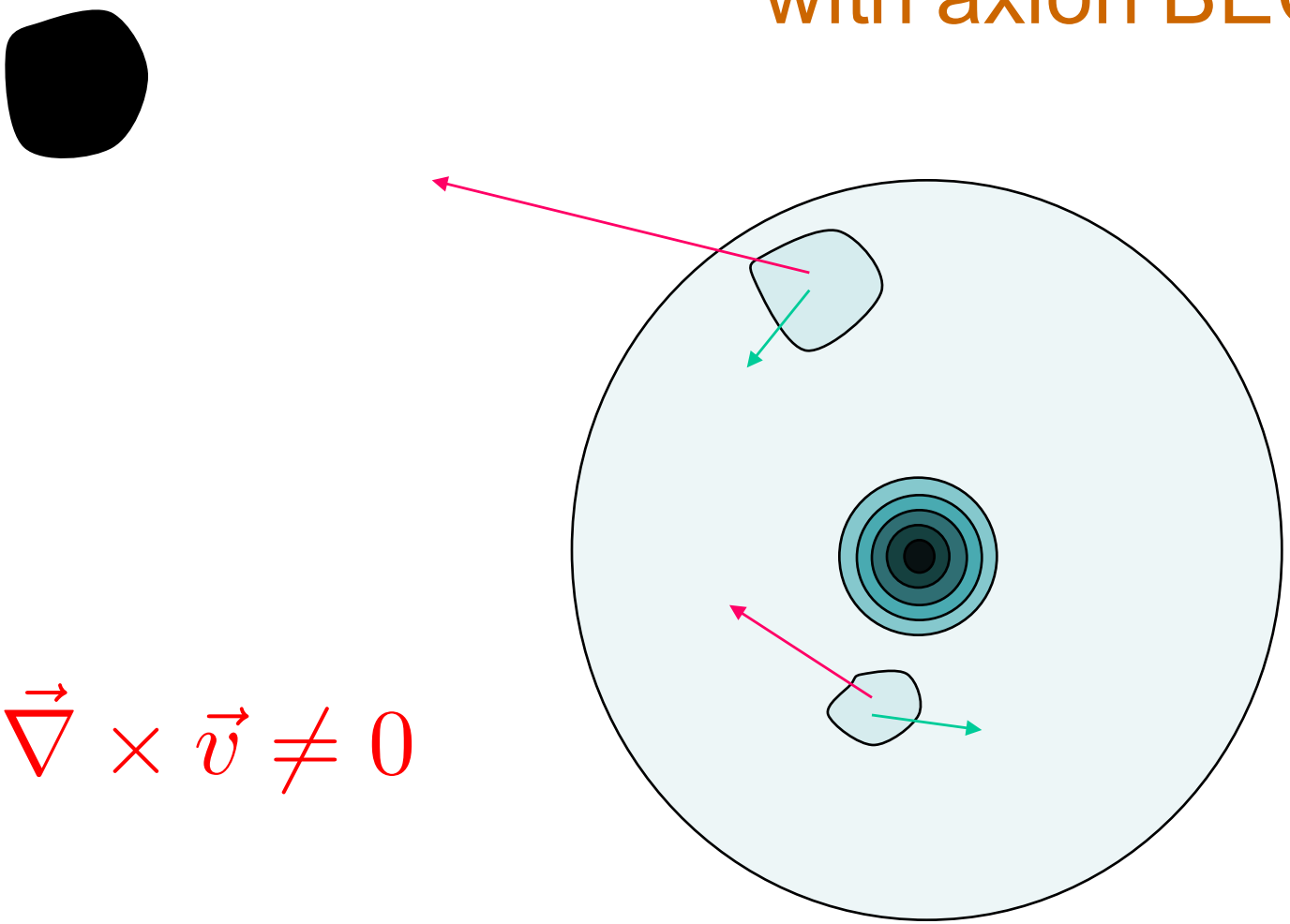

$$\vec{\nabla} \times \vec{v} \neq 0$$

in their lowest energy available state, the axions fall in with net overall rotation

Galactic halos have inner caustics as well as outer caustics.

If the initial velocity field is dominated by net overall rotation, the inner caustic is a ‘tricusp ring’.

If the initial velocity field is irrotational, the inner caustic has a ‘tent-like’ structure.

(Arvind Natarajan and PS, 2005).

simulation by Arvind Natarajan

in case of net overall rotation

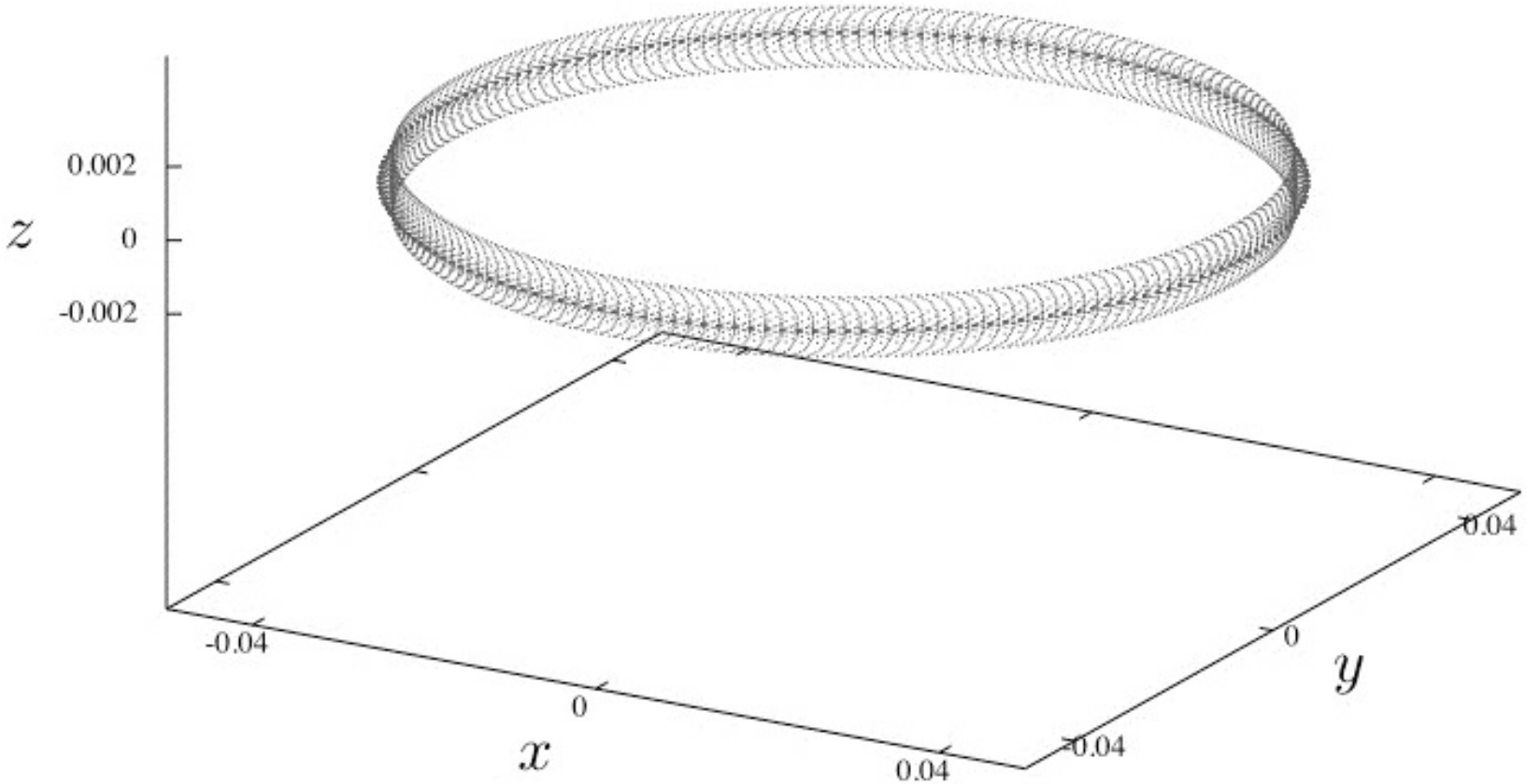

The caustic ring cross-section

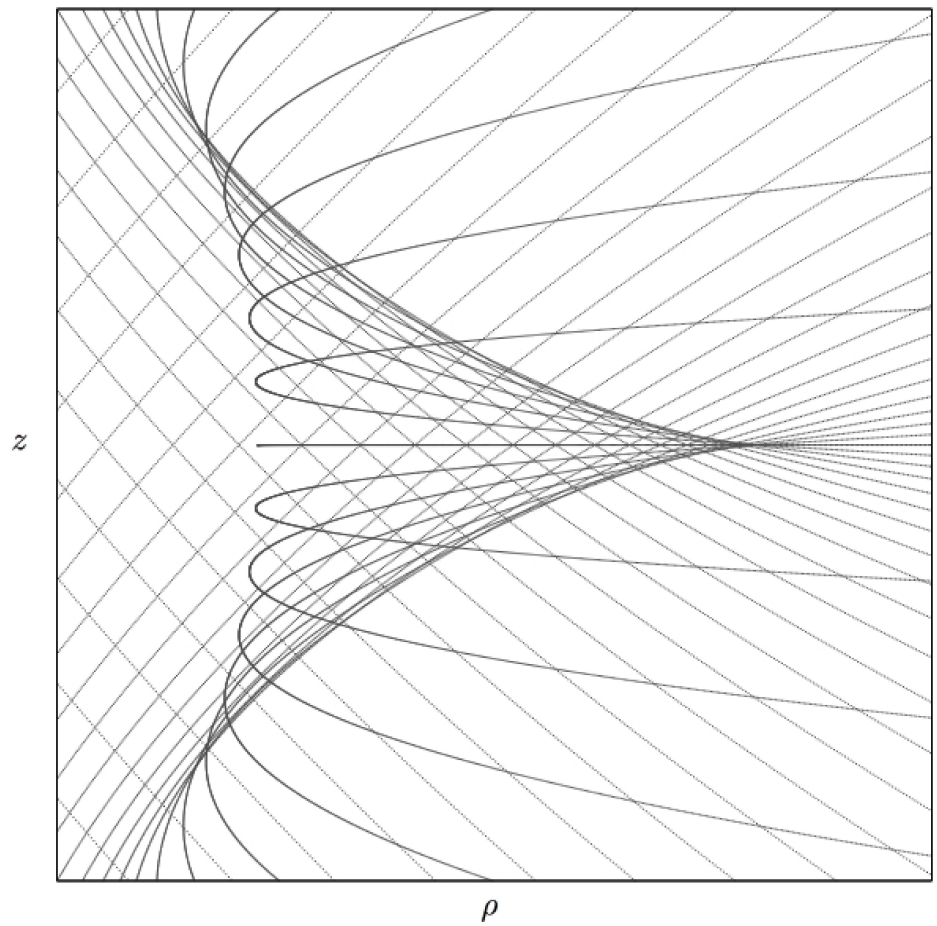

D_{-4}

an elliptic umbilic catastrophe

in case of irrotational flow

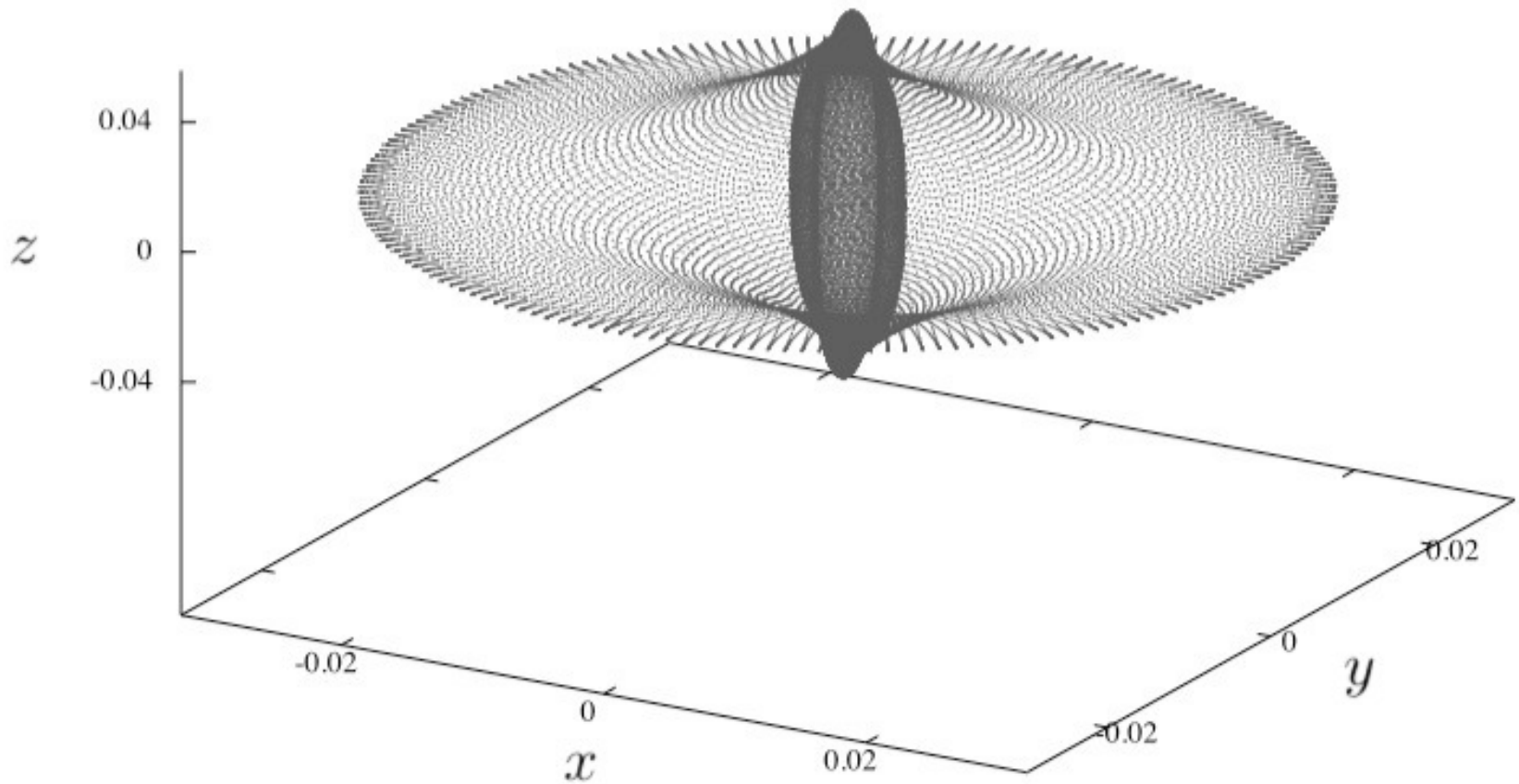

The caustic rings are predicted to be

in the galactic plane

with radii

$$(n = 1, 2, 3 \ldots)$$

$$a_n = \frac{40\text{kpc}}{n}\left(\frac{v_{rot}}{220\text{km/s}}\right)\left(\frac{j_{max}}{0.18}\right)$$

Axion Search Techniques

the cavity haloscope

the axion helioscope

shining light through walls

axion to magnon conversion

NMR methods

axion mediated long-range forces

LC circuit

atomic transitions

Axion dark matter is detectable

PS '83

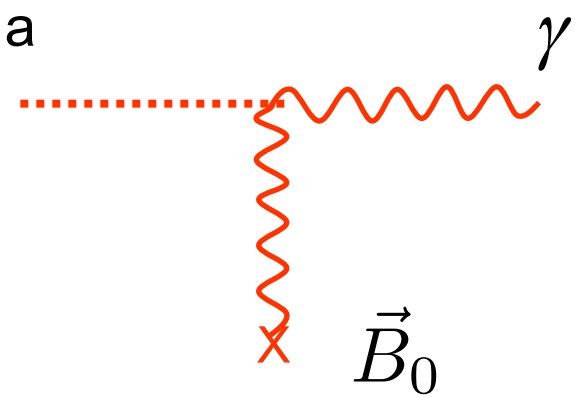

$$\mathcal{L}_{a\gamma\gamma} = g_\gamma \frac{a}{f_a} \vec{E} \cdot \vec{B}$$

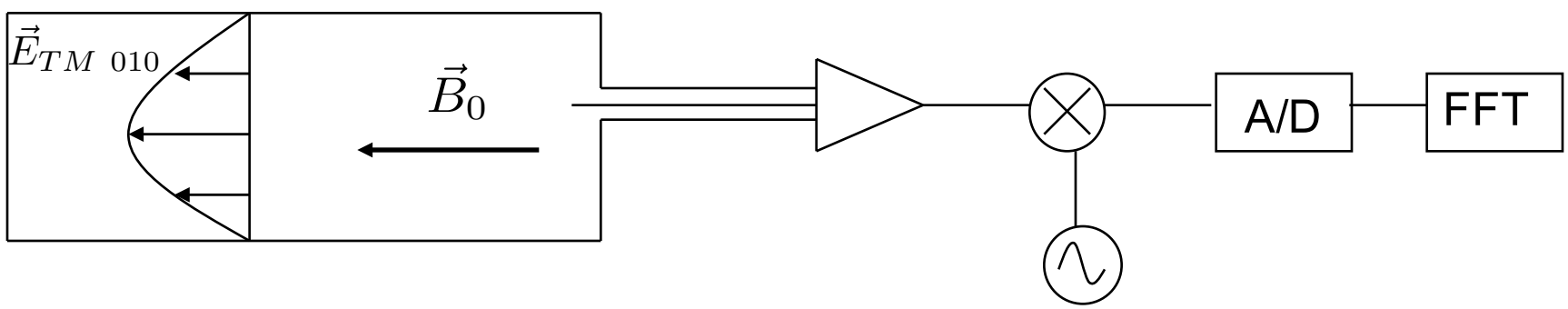

$$h\nu = m_a c^2 (1 + \frac{1}{2}\beta^2)$$

$$\beta = \frac{v}{c} \simeq 10^{-3}$$

$$Q_a \simeq 10^6$$

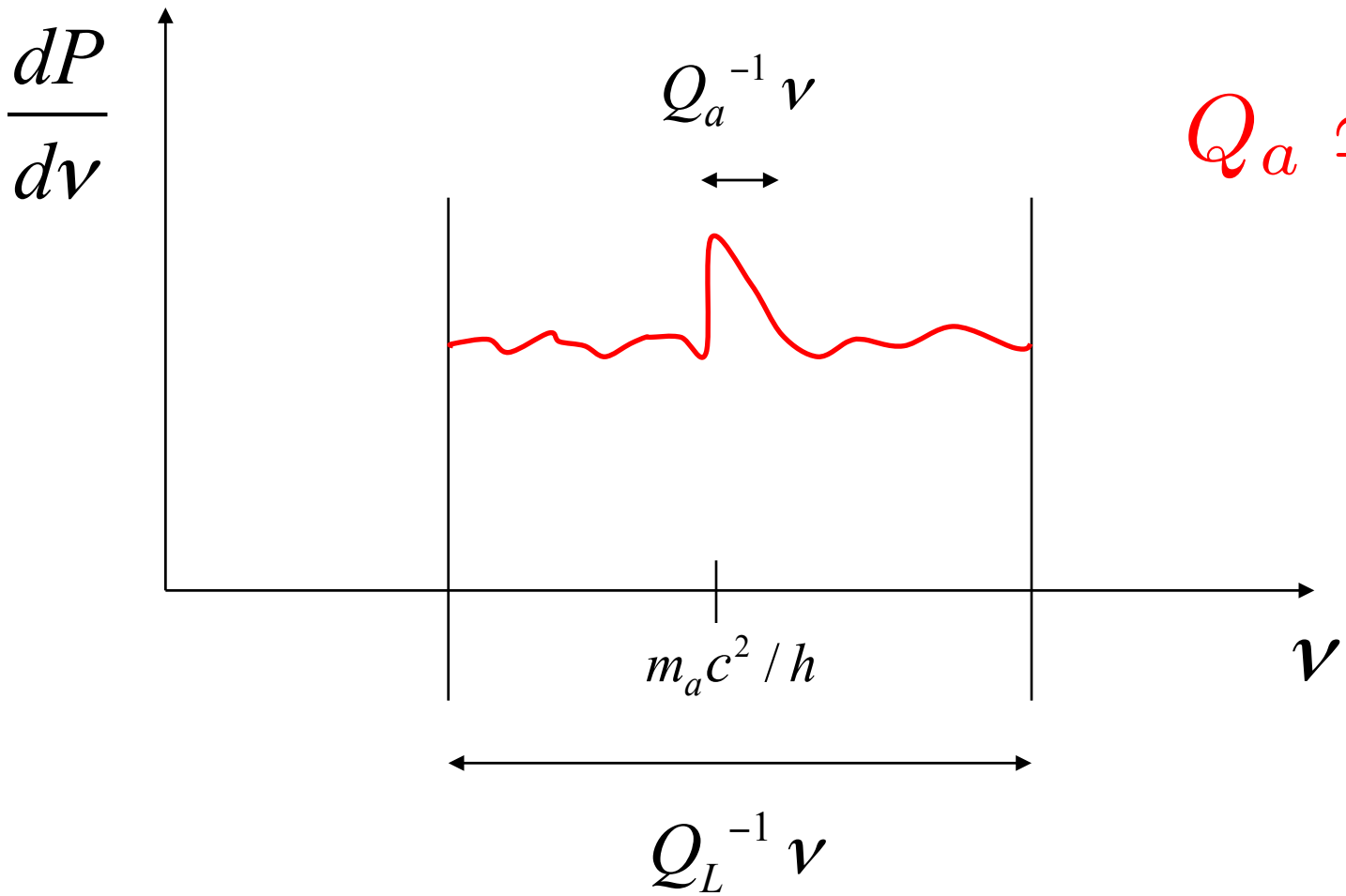

$a \rightarrow \gamma$

conversion power on resonance

$$P = \left(\frac{\alpha g_\gamma}{\pi f_a}\right)^2 V B_0^{\,2} \rho_a C m_a^{-1} Q_L$$

$$= 2 \cdot 10^{-22}\ \text{Watt} \left(\frac{V}{500\ \text{liter}}\right)\left(\frac{B_0}{7\ \text{Tesla}}\right)^2 \left(\frac{C}{0.4}\right)$$

$$\left(\frac{g_\gamma}{0.36}\right)^2 \left(\frac{\rho_a}{5 \cdot 10^{-25}\ \text{gr/cm}^3}\right)\left(\frac{m_a c^2}{h\ \text{GHz}}\right)\left(\frac{Q_L}{10^5}\right)$$

search rate for s/n = 4

$$\frac{df}{dt} = \frac{1.2\ \text{GHz}}{\text{year}} \left(\frac{P}{2 \cdot 10^{-22}\ \text{Watt}}\right)^2 \left(\frac{3\ K}{T_n}\right)^2$$

Axion Dark Matter eXperiment

Magnet with Insert (side view)

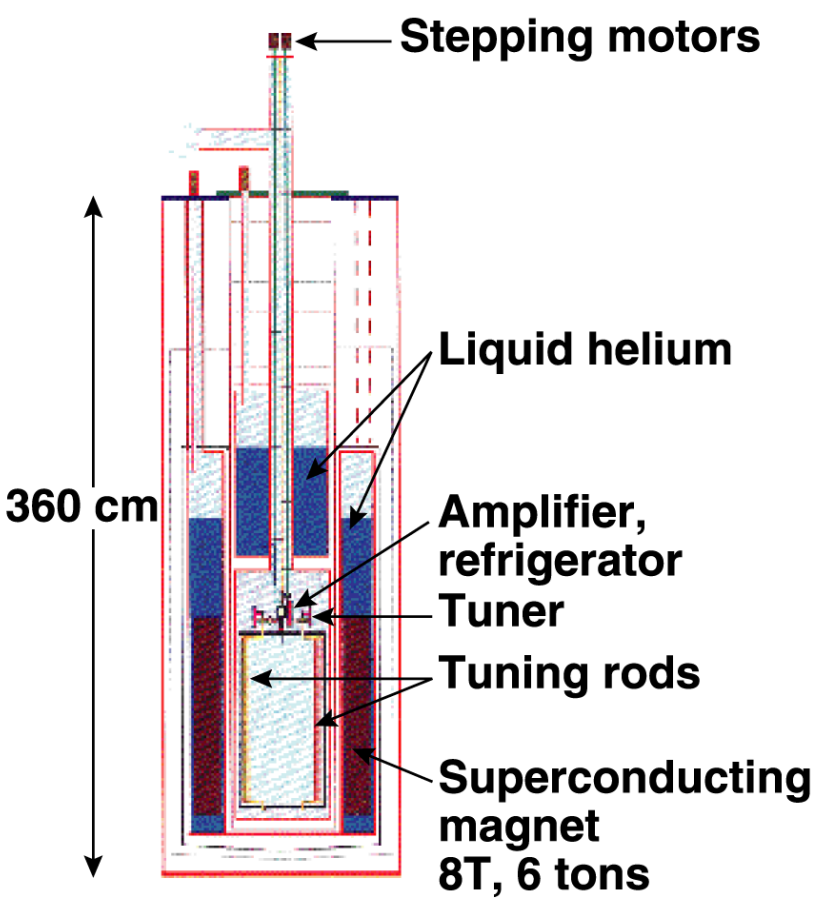

Pumped LHe → T ~ 1.5 k

Magnet

8 T, 1 m × 60 cm ∅

ADMX hardware

high Q cavity

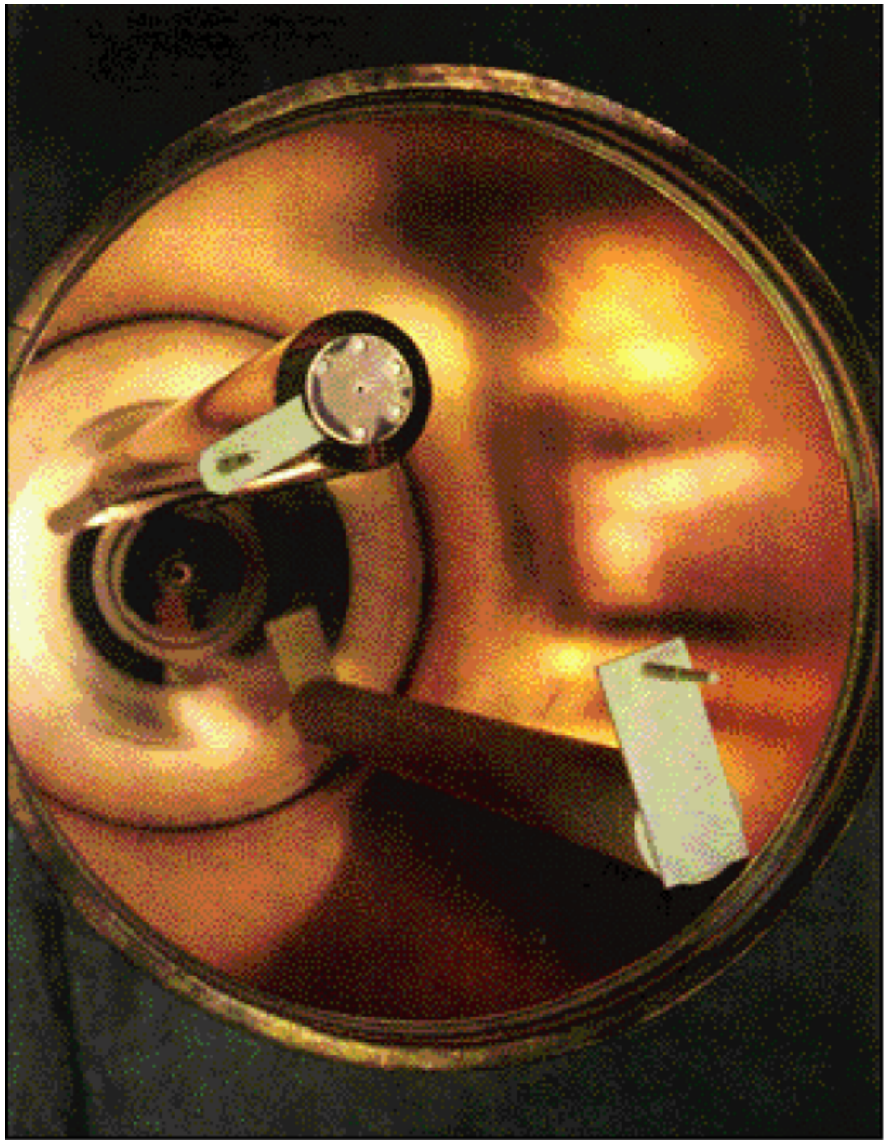

experimental insert

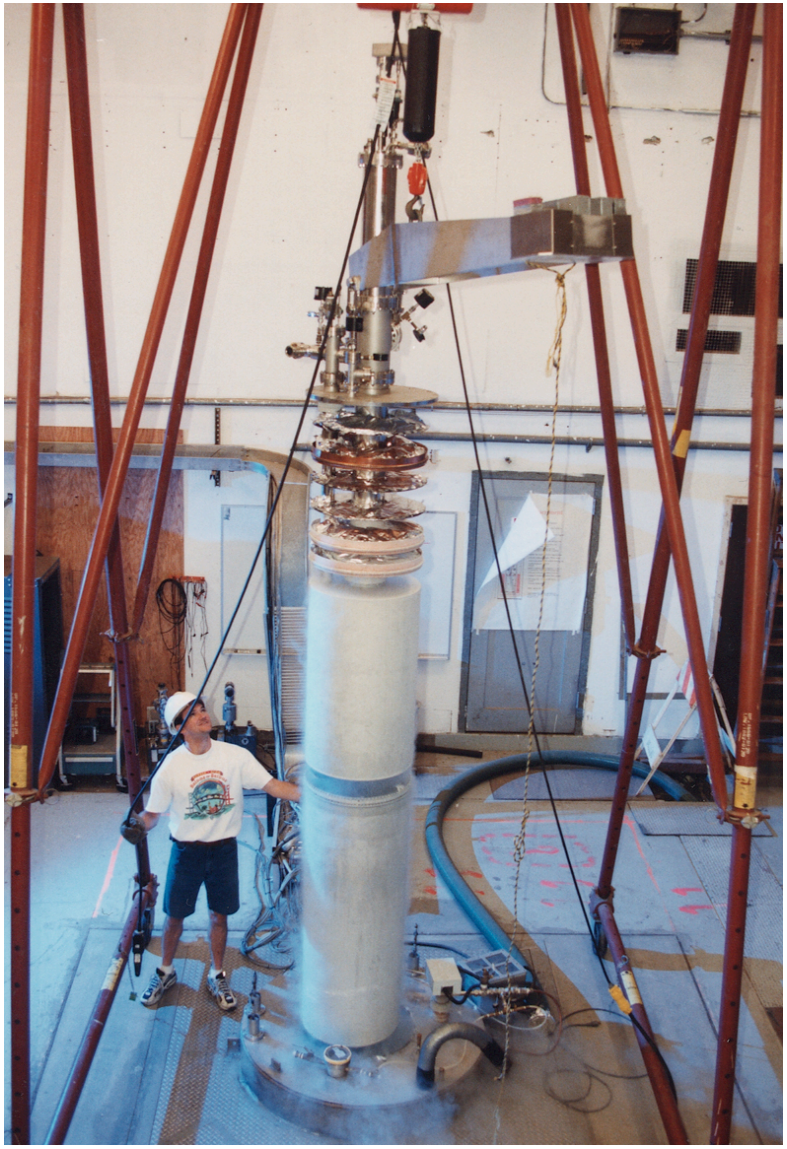

ADMX in its second generation

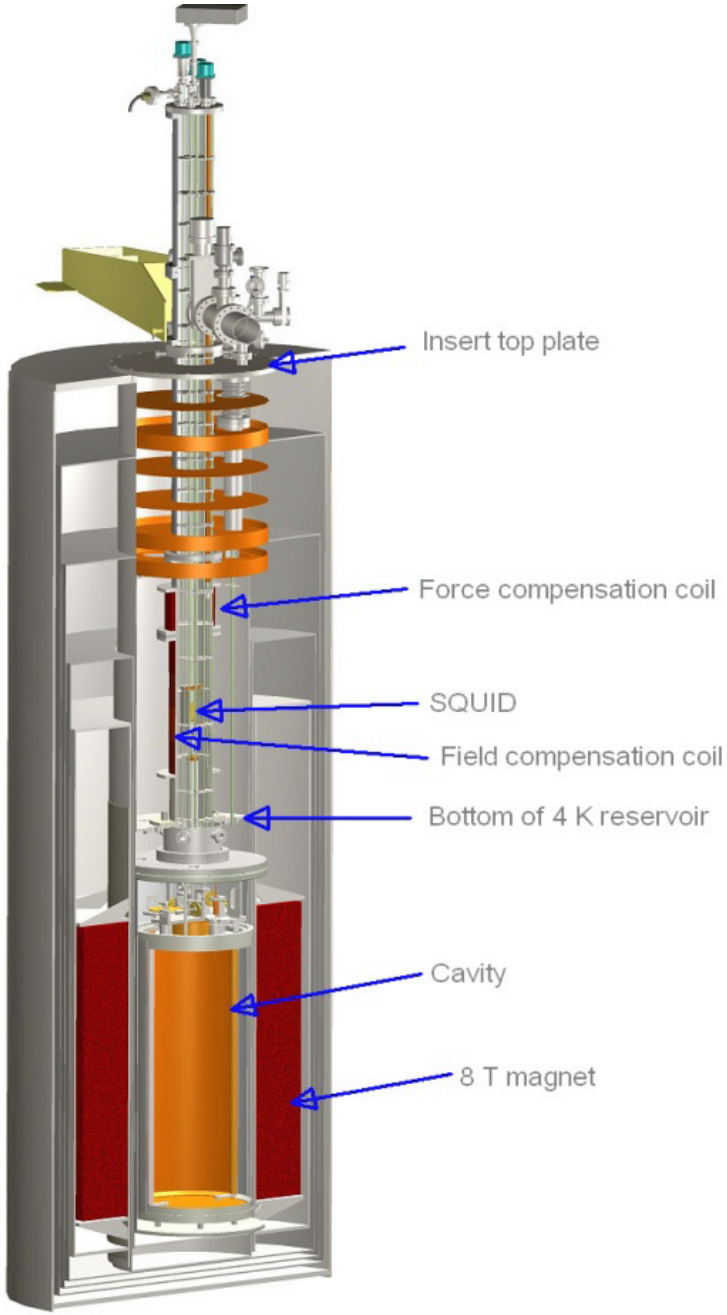

*Supported by DOE Grants DE-FG02-97ER41029, DE-FG02-96ER40956, DE-AC52-07NA27344, DE-AC03-76SF00098, NSF Grant PHY-1067242, and the Livermore LDRD program

Upgrade with SQUID Amplifiers

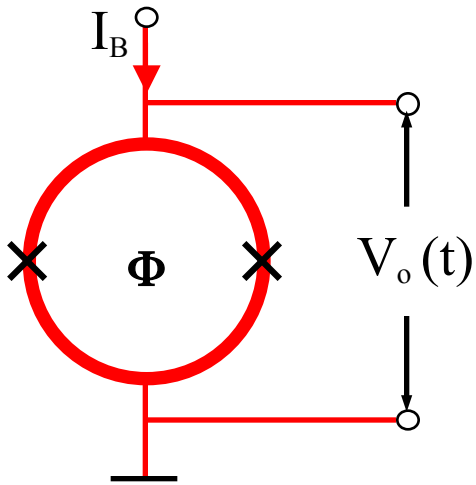

The basic SQUID amplifier is a flux-to-voltage transducer

SQUID noise arises from Nyquist noise in shunt resistance scales linearly with T

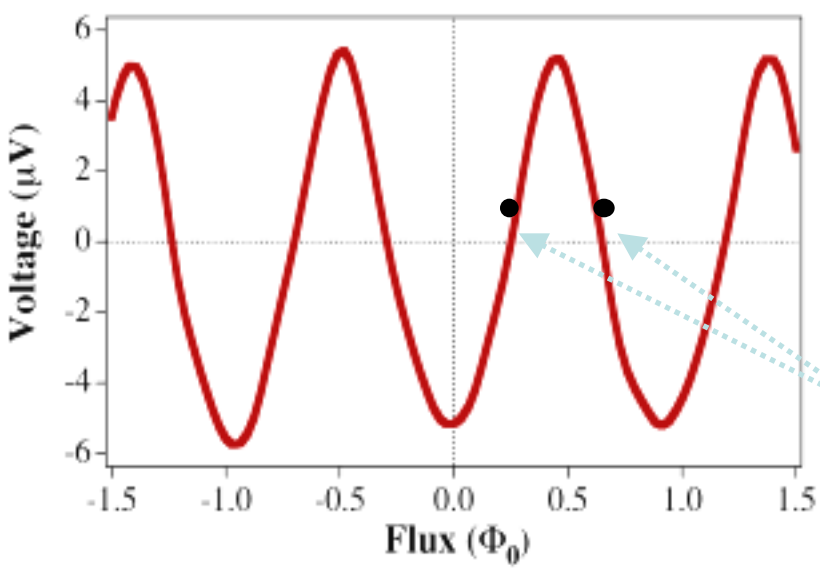

However, SQUIDs of conventional design are poor amplifiers above 100 MHz (parasitic couplings).

Flux-bias to here

Quantum-limited SQUID-based amplification

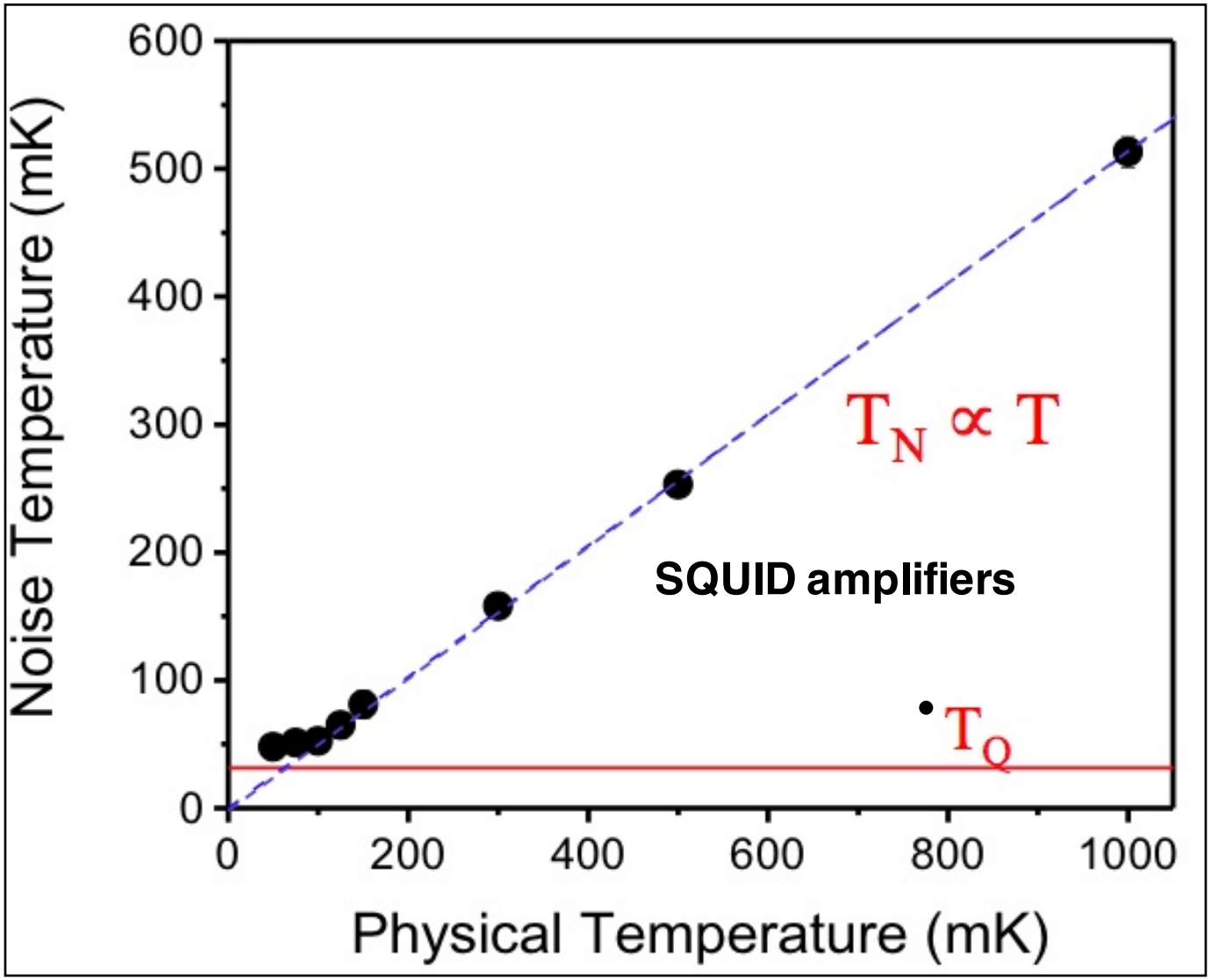

- SQUIDs have been measured with $T_N \sim 50$ mK
- Compared to ~ 2 K for HFET amplifiers
- Near quantum– limited noise
- Provides a large increase in ADMX sensitivity

J. Clarke et al.

Gen 2 ADMX sensitivity

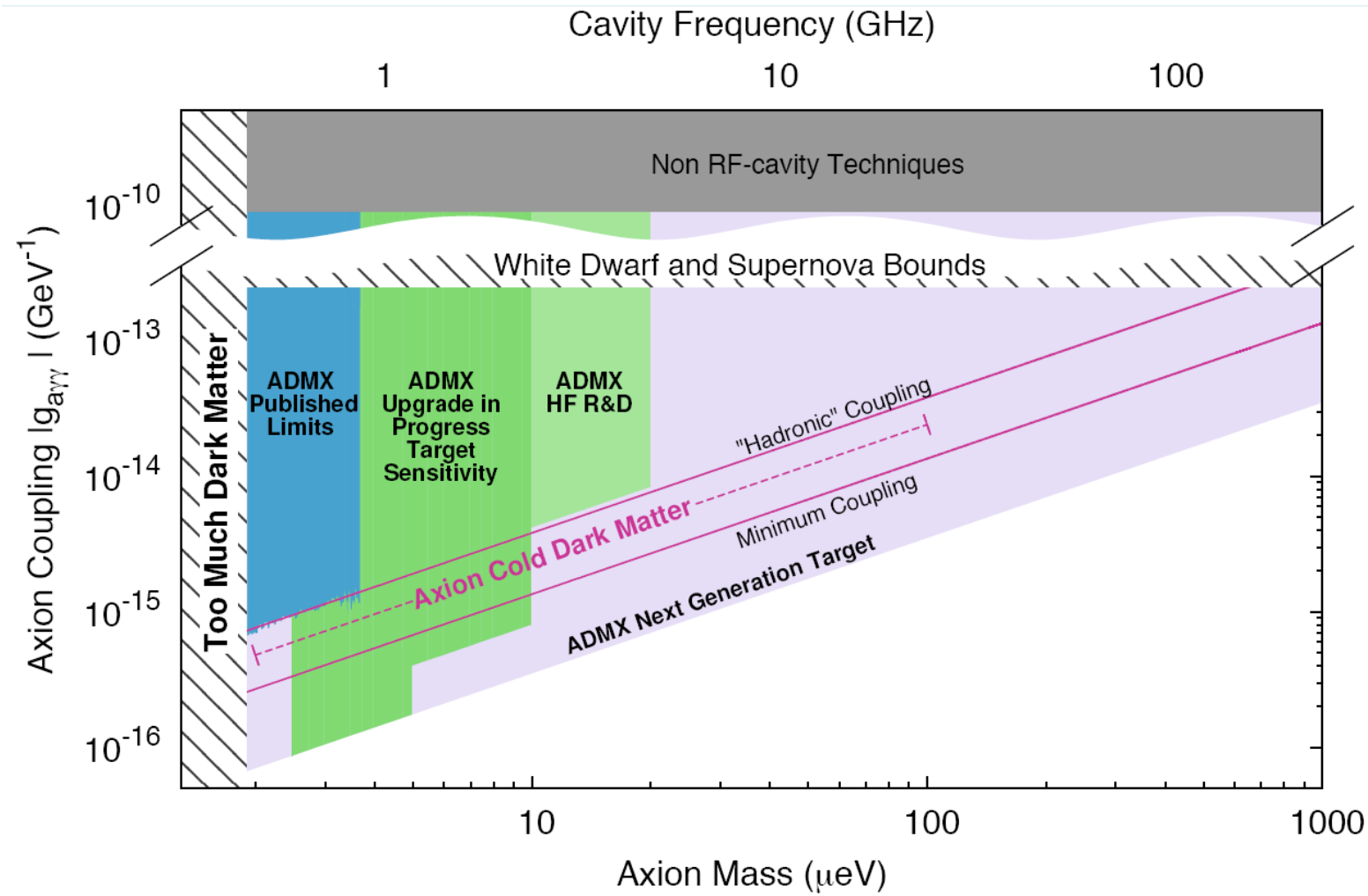

Will scan the lower-mass decade at or below DFSZ sensitivity

ADMX-HF at Yale

- Multi-post system that consists of 3 rotors connected on common axis and 3 stators.
- 4” ID cavity: Six 0.5” diameter rods
- Freq. span 4.7- 6.0 GHz

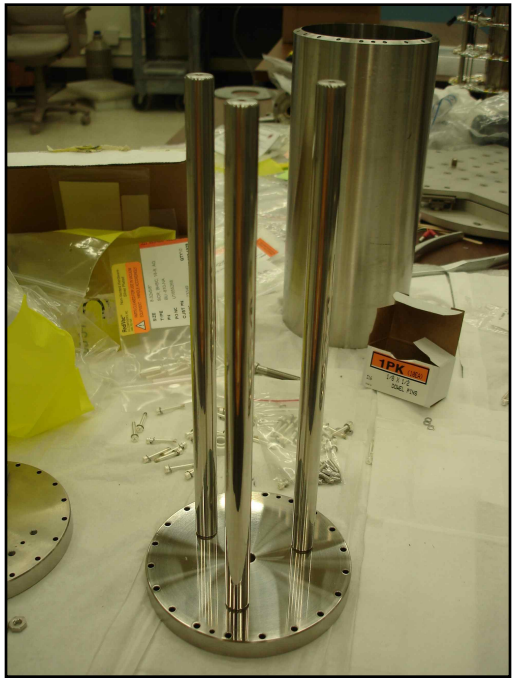

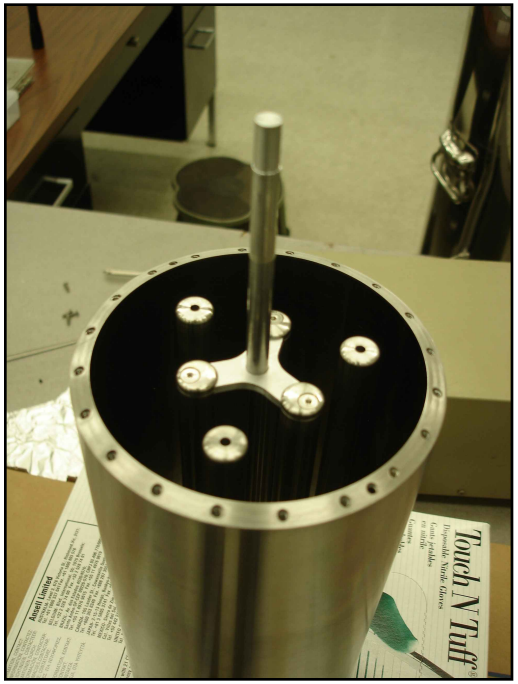

B. Brubaker et al., arXiv: 1610.02580

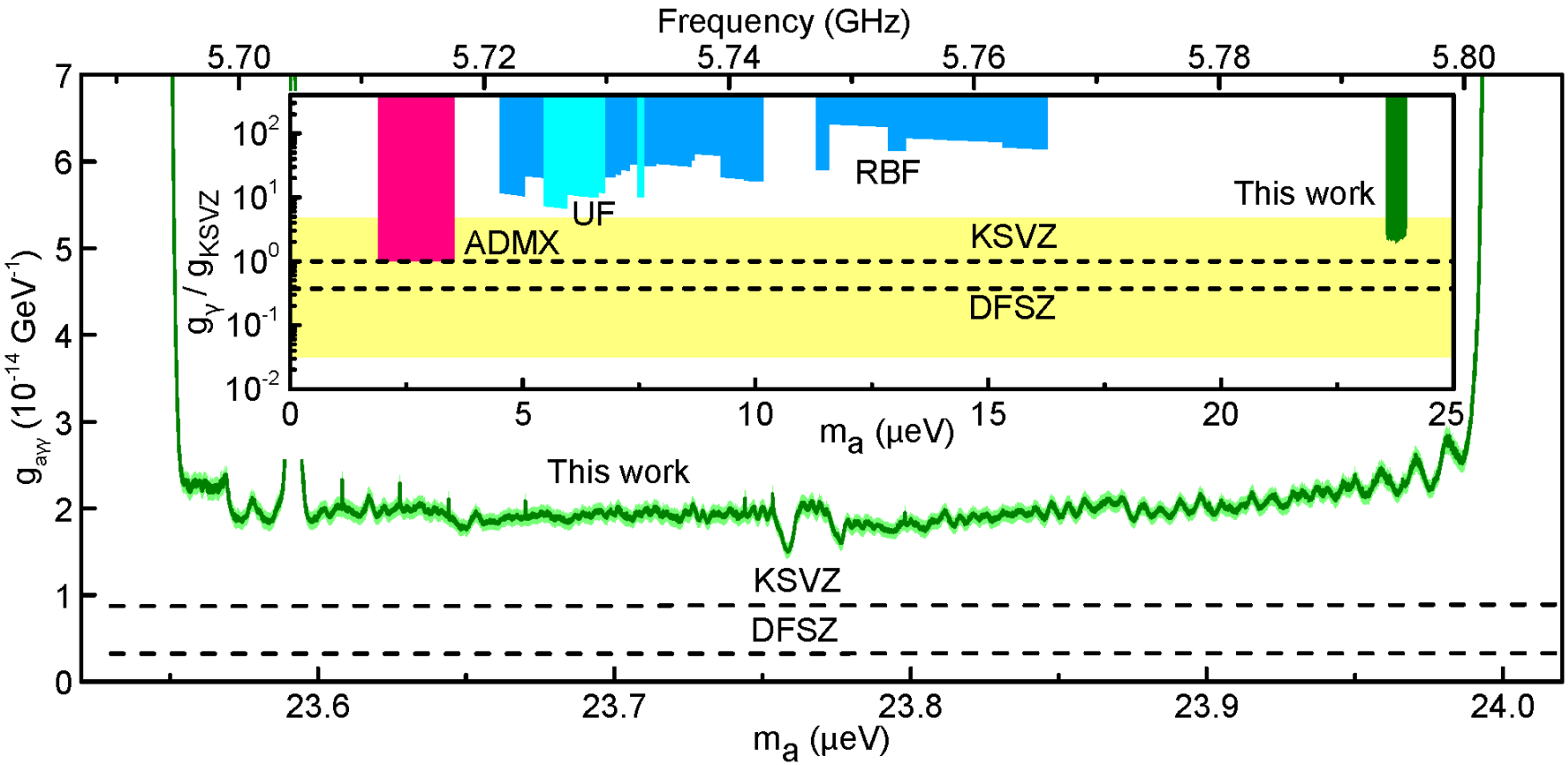

FIG. 3. Our exclusion limit at 90% confidence. The light green shaded region is a 1σ error band. The large notch around 5.704 GHz is the result of cutting spectra around a previously unidentified intruder mode. The narrow notches correspond to frequencies where synthetic axion signals were injected in one of the scans. The inset shows our results (green) together with previous cavity limits from ADMX (magenta, [7]) and early experiments at Brookhaven (RBF, blue, [18]) and the University of Florida (UF, cyan, [19]). The axion model band [13] is shown in yellow.

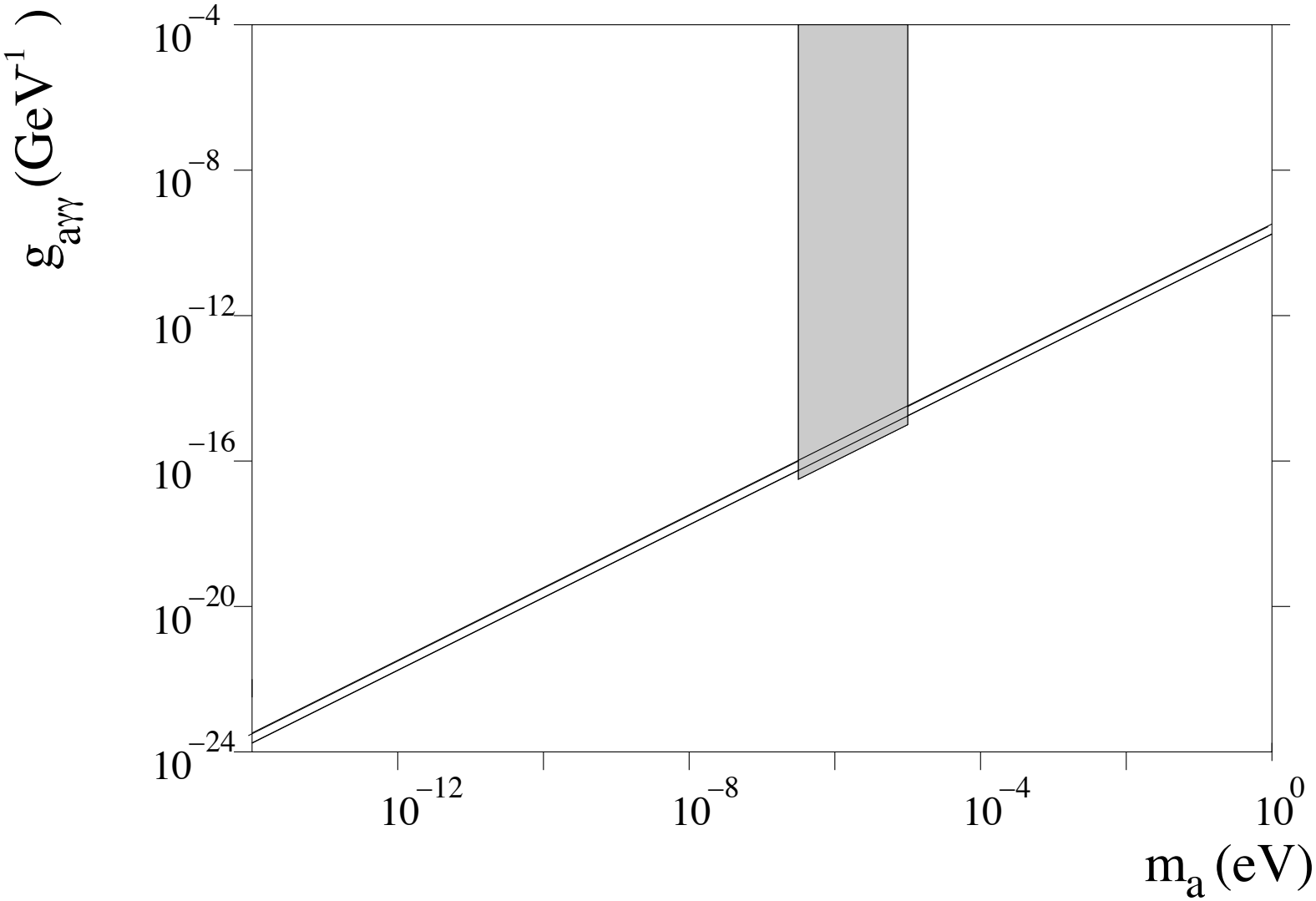
$g_{a\gamma\gamma}$ (GeV^{1})
10^{-4}
10^{-8}
10^{-12}
10^{-16}
10^{-20}
10^{-24}
10^{-12}
10^{-8}
10^{-4}
10^{0}
m_a (eV)

Axion to photon conversion in a magnetic field

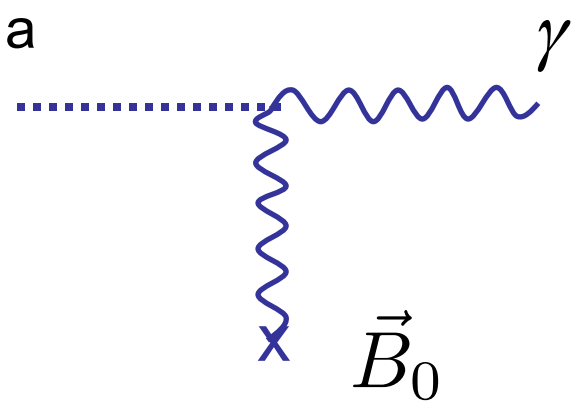

conversion probability

$$p(a \longleftrightarrow \gamma) = \left(\frac{\alpha\, g_\gamma}{\pi\, f_a}\right)^2 \mathrm{B}_0{}^2 \left(\frac{\sin\frac{q_z L}{2}}{q_z}\right)^2$$

with $$q_z = \frac{m_a{}^2 - \omega_{\mathrm{pl}}{}^2}{2E_a}$$

Theory

- P. S. ’83
- L. Maiani, R. Petronzio and E. Zavattini ’86
- K. van Bibber et al. ’87
- G. Raffelt and L. Stodolsky, ‘88
- K. van Bibber et al. ’89

Experiment

- D. Lazarus et al. ’92
- R. Cameron et al. ‘93
- S. Moriyama et al. ’98, Y. Inoue et al. ’02
- K. Zioutas et al. 04
- E. Zavattini et al. 05

Tokyo Axion Helioscope

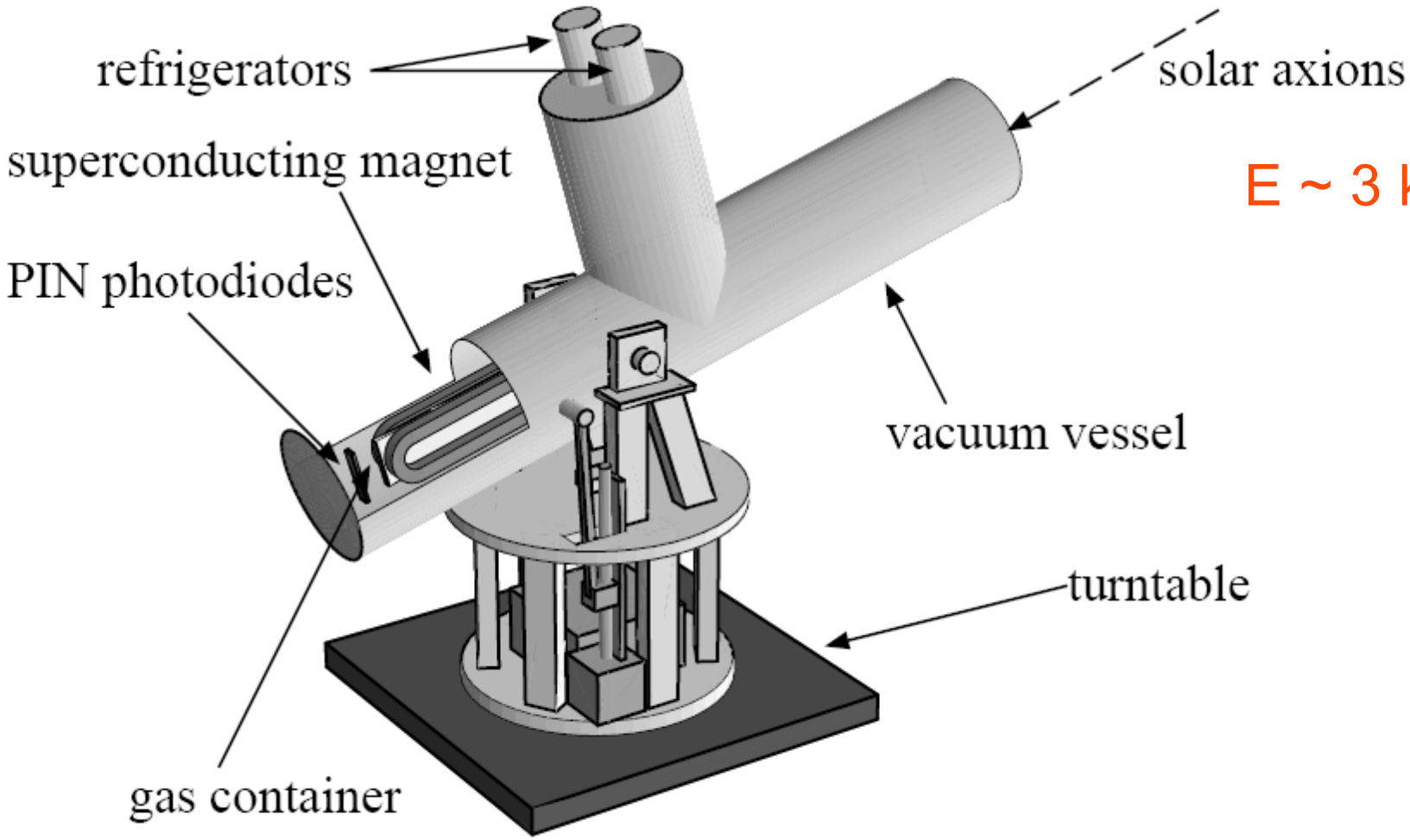

E ~ 3 keV

Cern Axion Solar Telescope

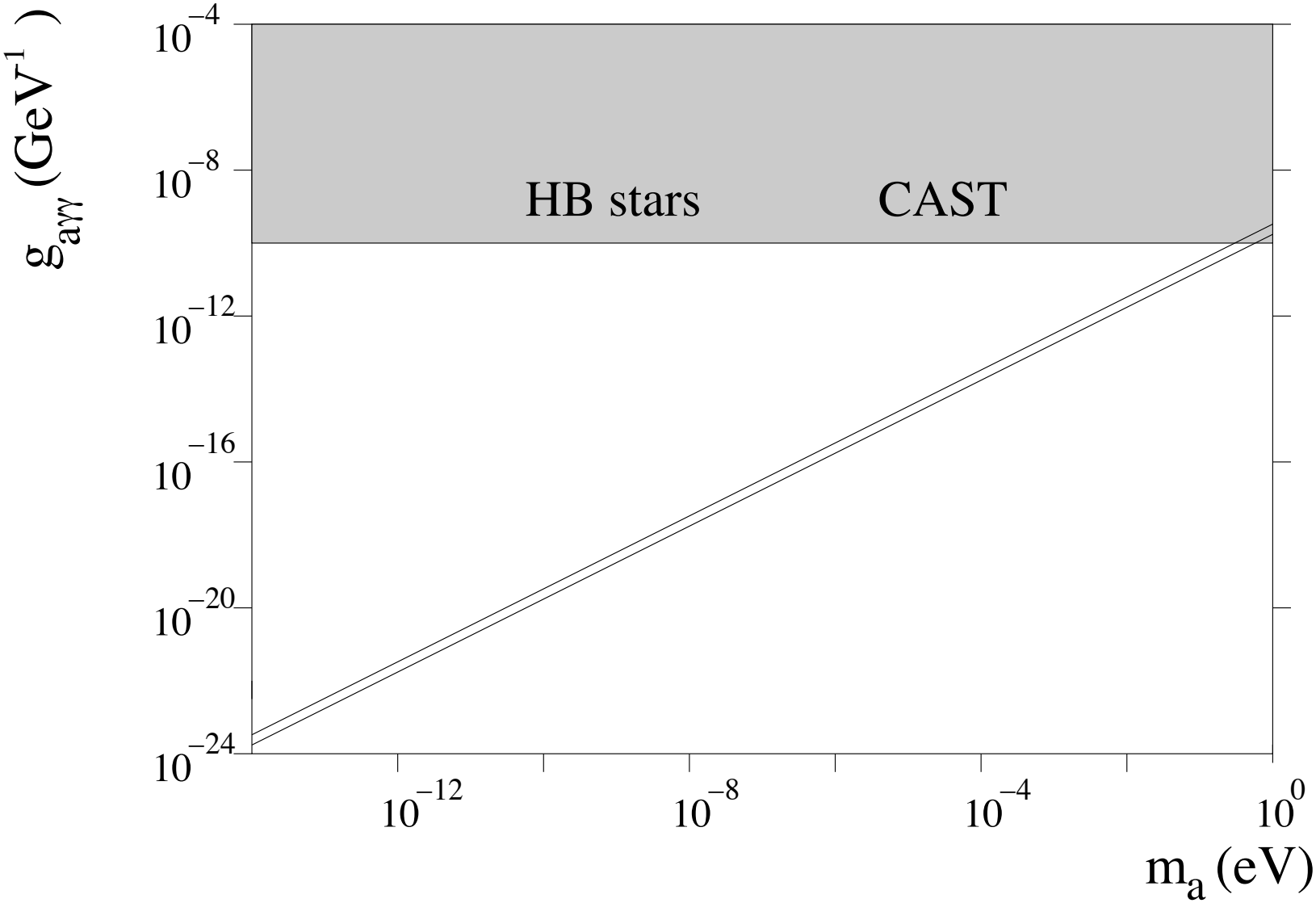
$g_{a\gamma\gamma}$ (GeV^{-1})
10^{-4}
10^{-8}
10^{-12}
10^{-16}
10^{-20}
10^{-24}
HB stars
CAST
10^{-12}
10^{-8}
10^{-4}
10^{0}
m_a (eV)

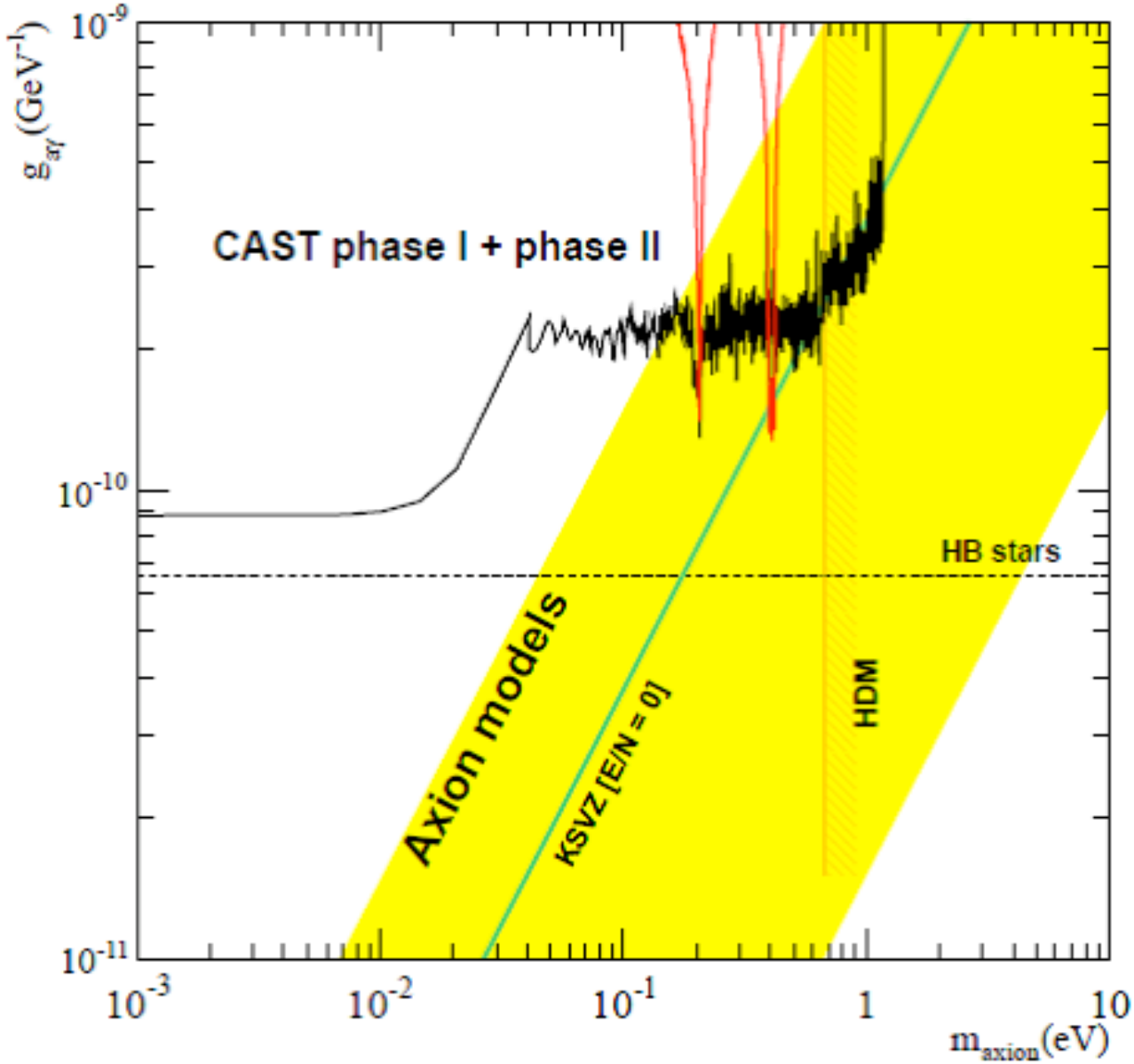

CAST Collaboration: Phys. Rev. Lett. 112 (2013) 091302

IAXO – Conceptual Design

- Large toroidal 8-coil magnet L = ~20 m
- 8 bores: 600 mm diameter each
- 8 x-ray optics + 8 detection systems
- Rotating platform with services

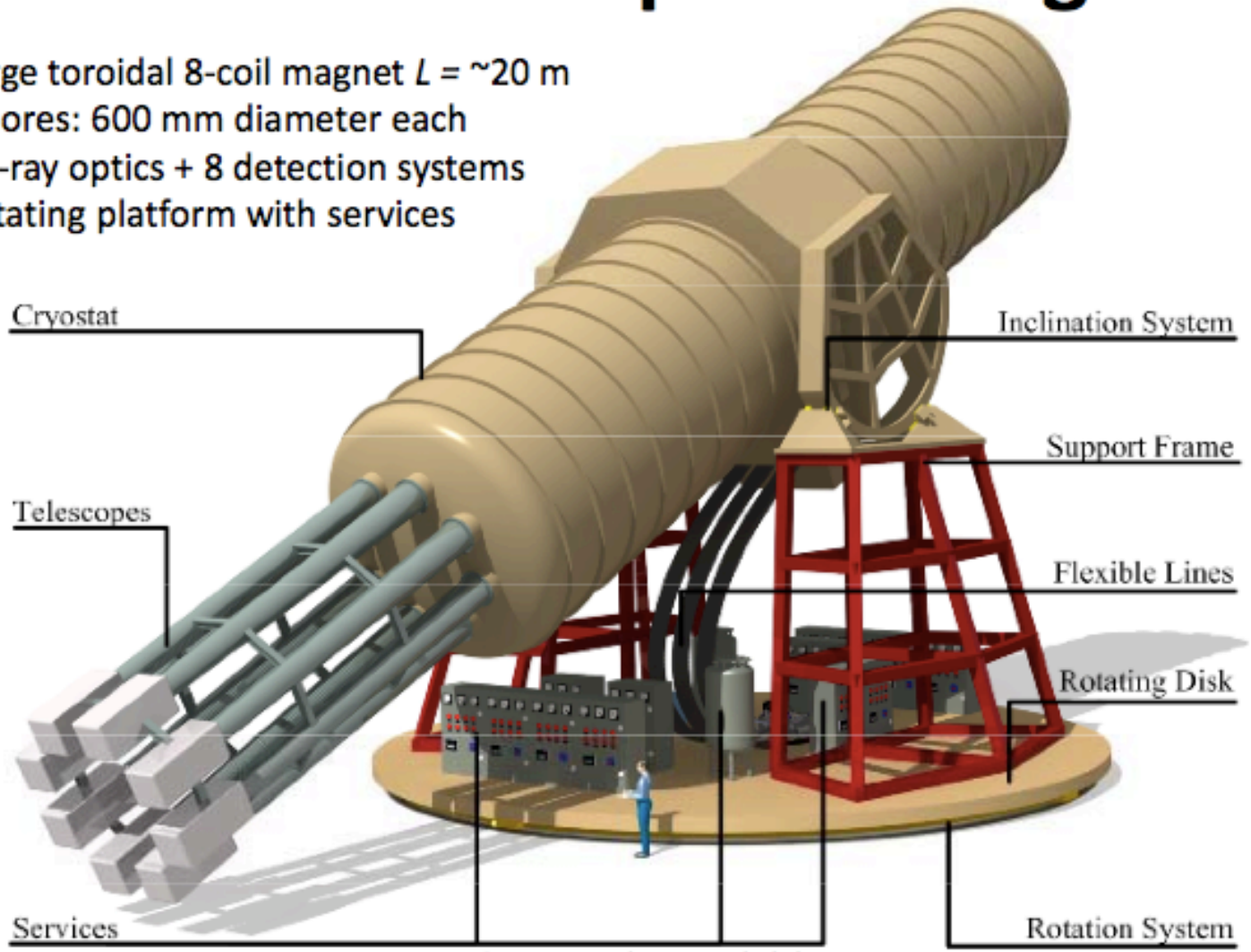

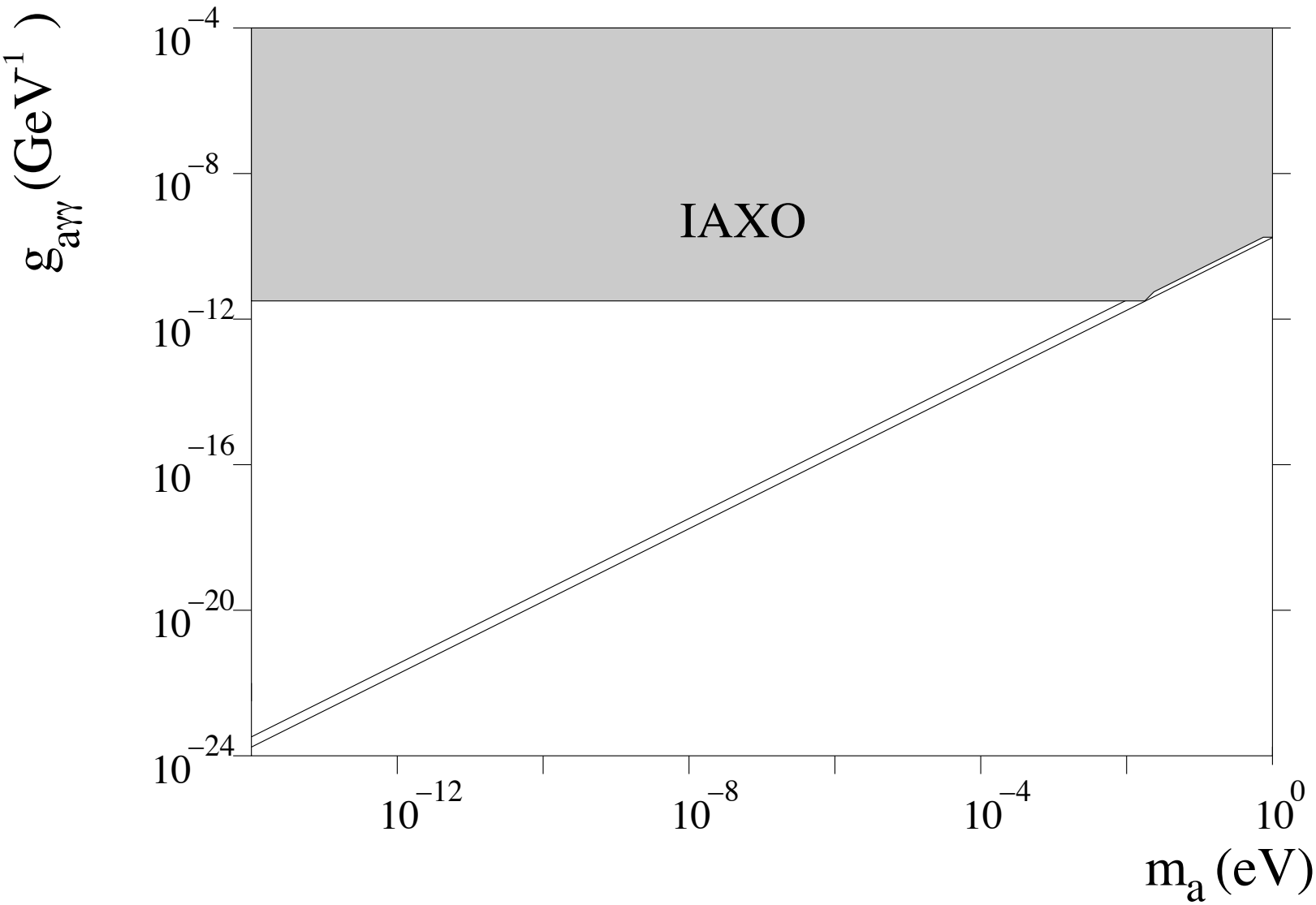
IAXO
$g_{a\gamma\gamma}$ (GeV^{-1})
10^{-4}
10^{-8}
10^{-12}
10^{-16}
10^{-20}
10^{-24}
10^{-12}
10^{-8}
10^{-4}
10^{0}
m_a (eV)

Shining light through walls

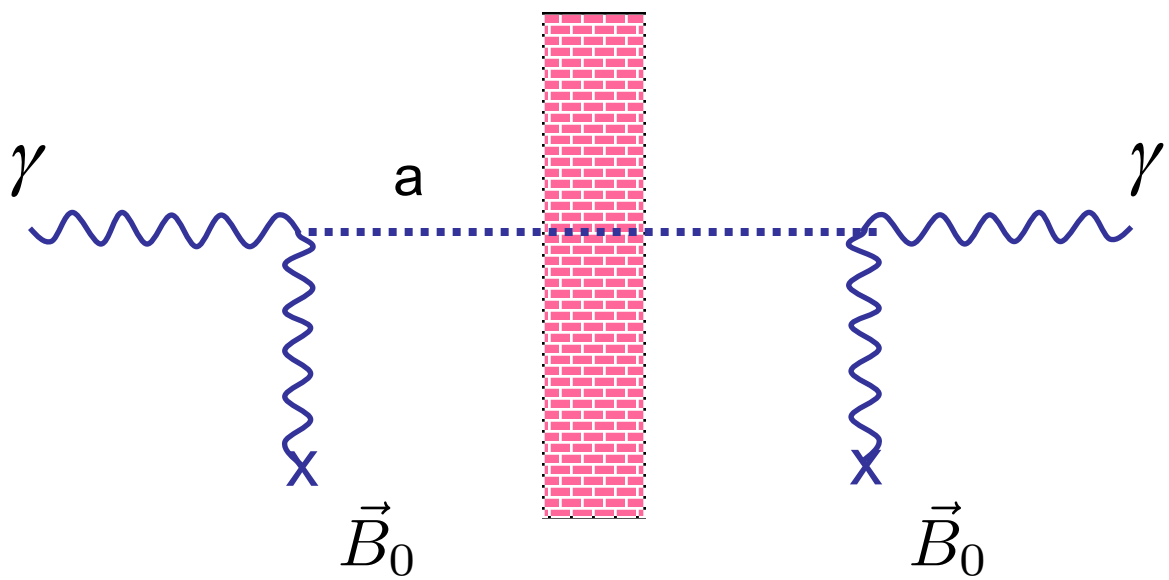

rate $\propto \dfrac{1}{f_a^{\,4}}$

K. van Bibber et al. ‘87

A. Ringwald ‘03

R. Rabadan,
A. Ringwald and
C. Sigurdson ‘05

P. Pugnat et al. '05

C. Robilliard et al. '07

A. Afanasev et al. '08

A. Chou et al. '08

K. Ehret et al. '10

Limits from "light through wall" axion searches

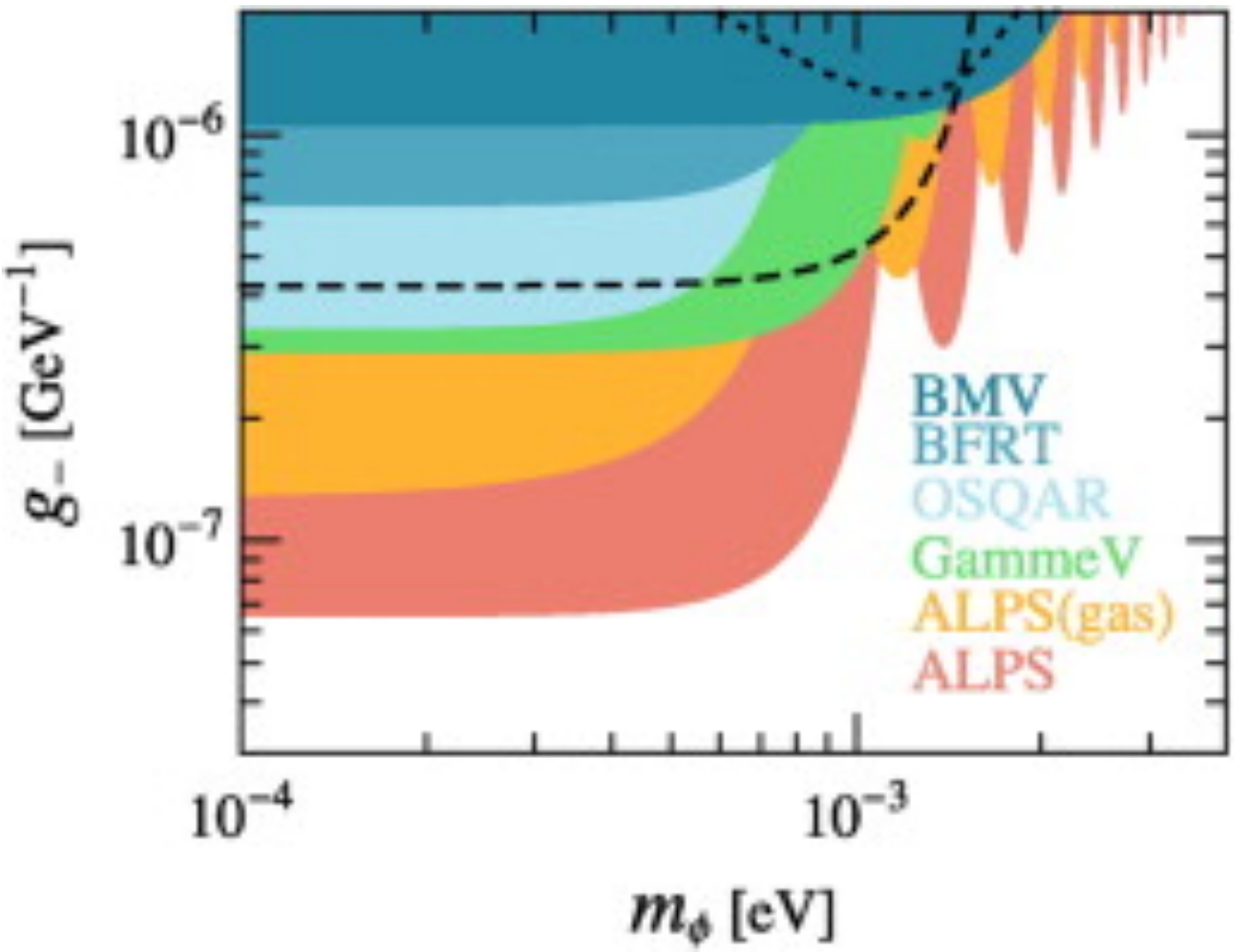

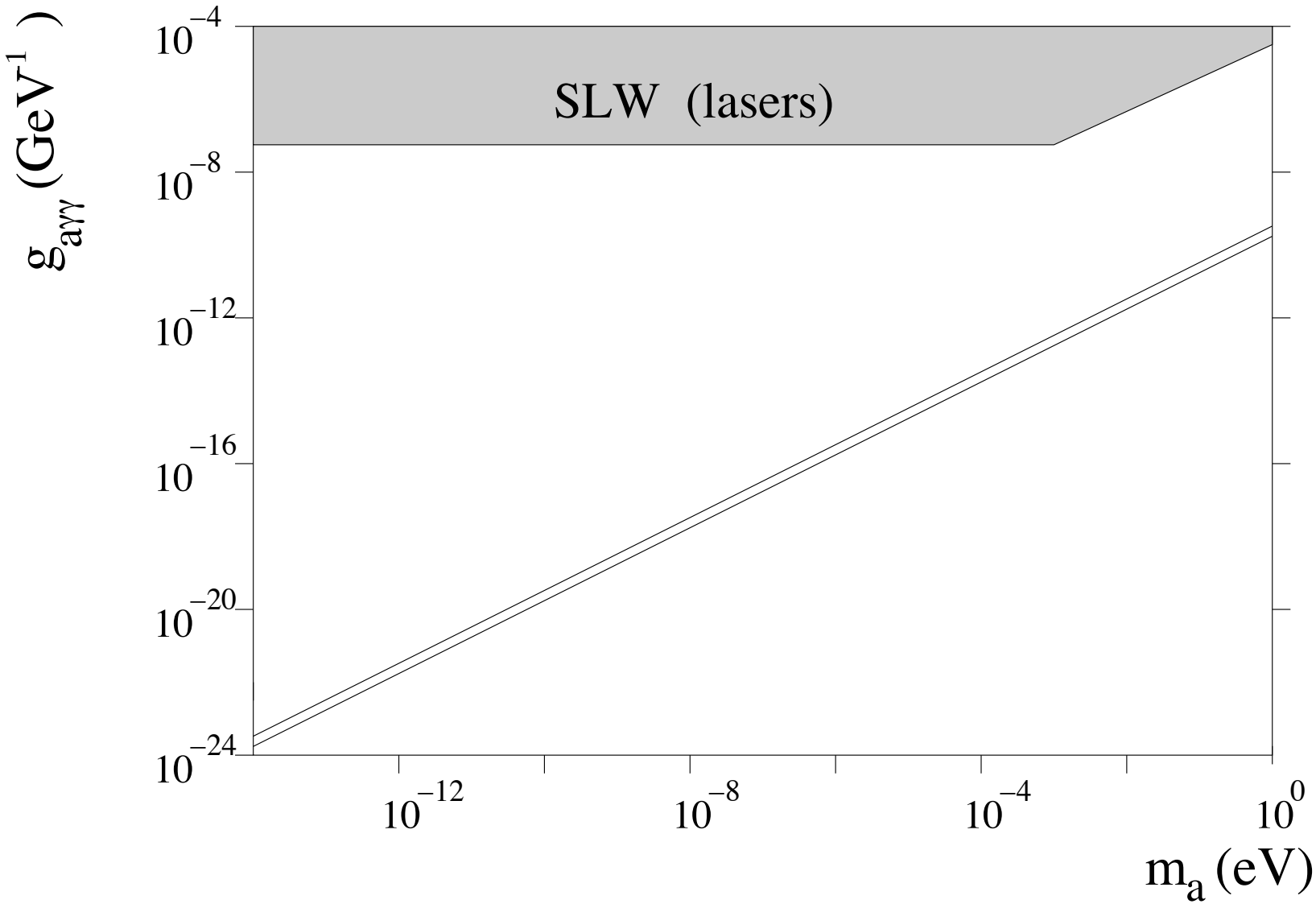
SLW (lasers)
$g_{a\gamma\gamma}$ (GeV^{1})
10^{-4}
10^{-8}
10^{-12}
10^{-16}
10^{-20}
10^{-24}
10^{-12}
10^{-8}
10^{-4}
10^{0}
m_a (eV)

Resonantly Enhanced Axion-Photon Regeneration

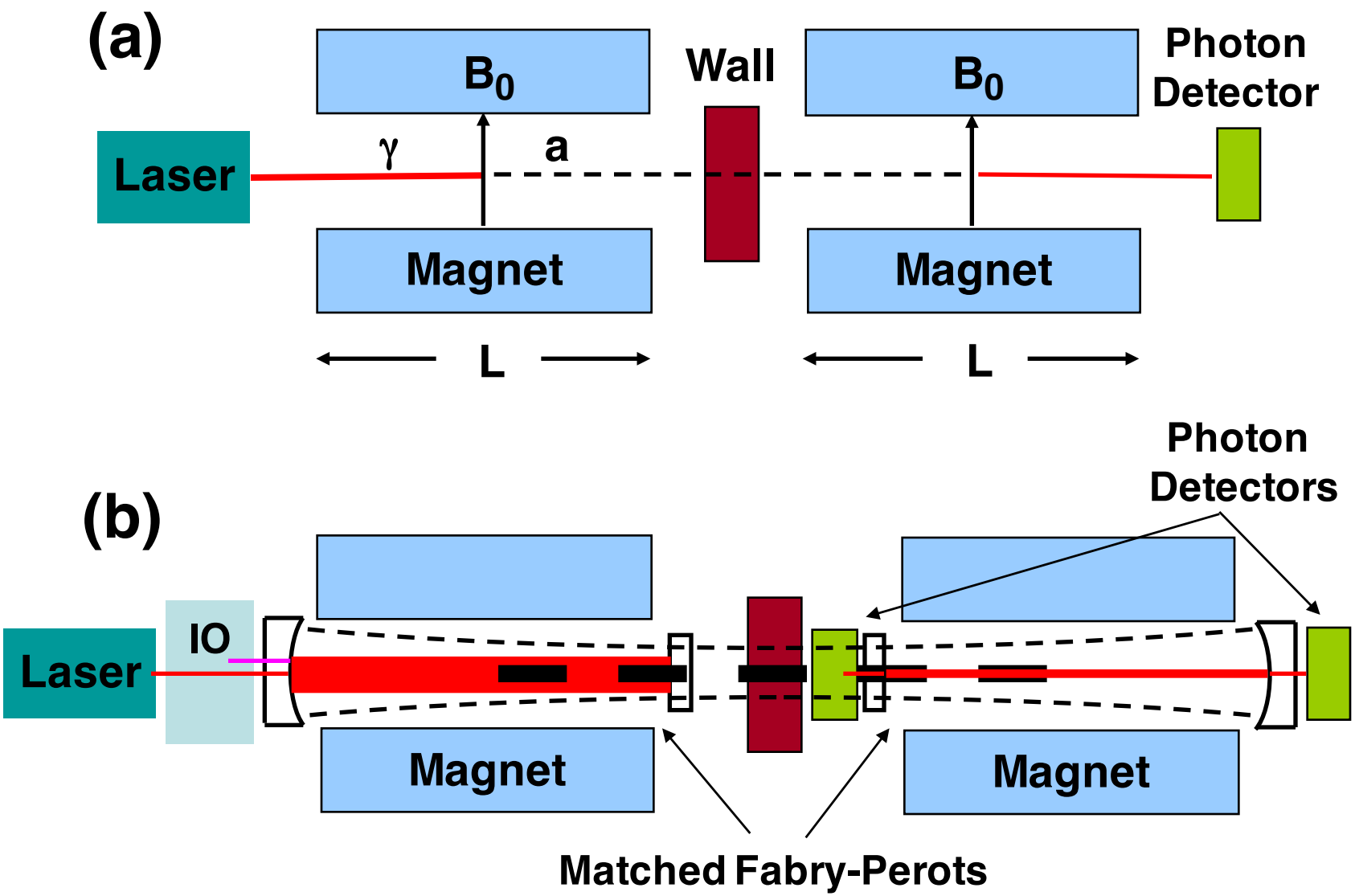

F. Hoogeveen (1996); P.S., D. Tanner and K. van Bibber (2007)

ALPS II at DESY

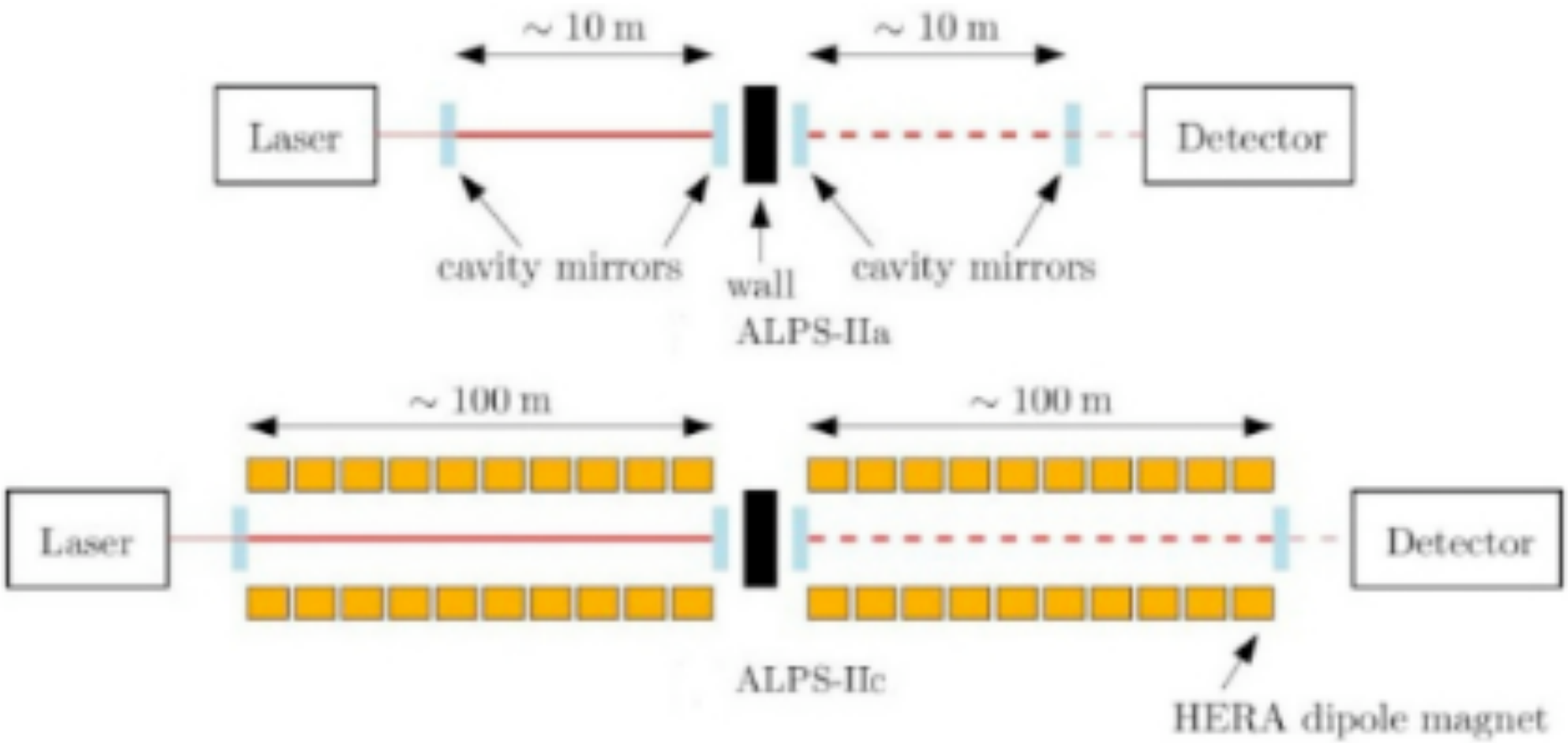

Expected sensitivity : $2 \cdot 10^{-11}\ \mathrm{GeV}^{-1}$

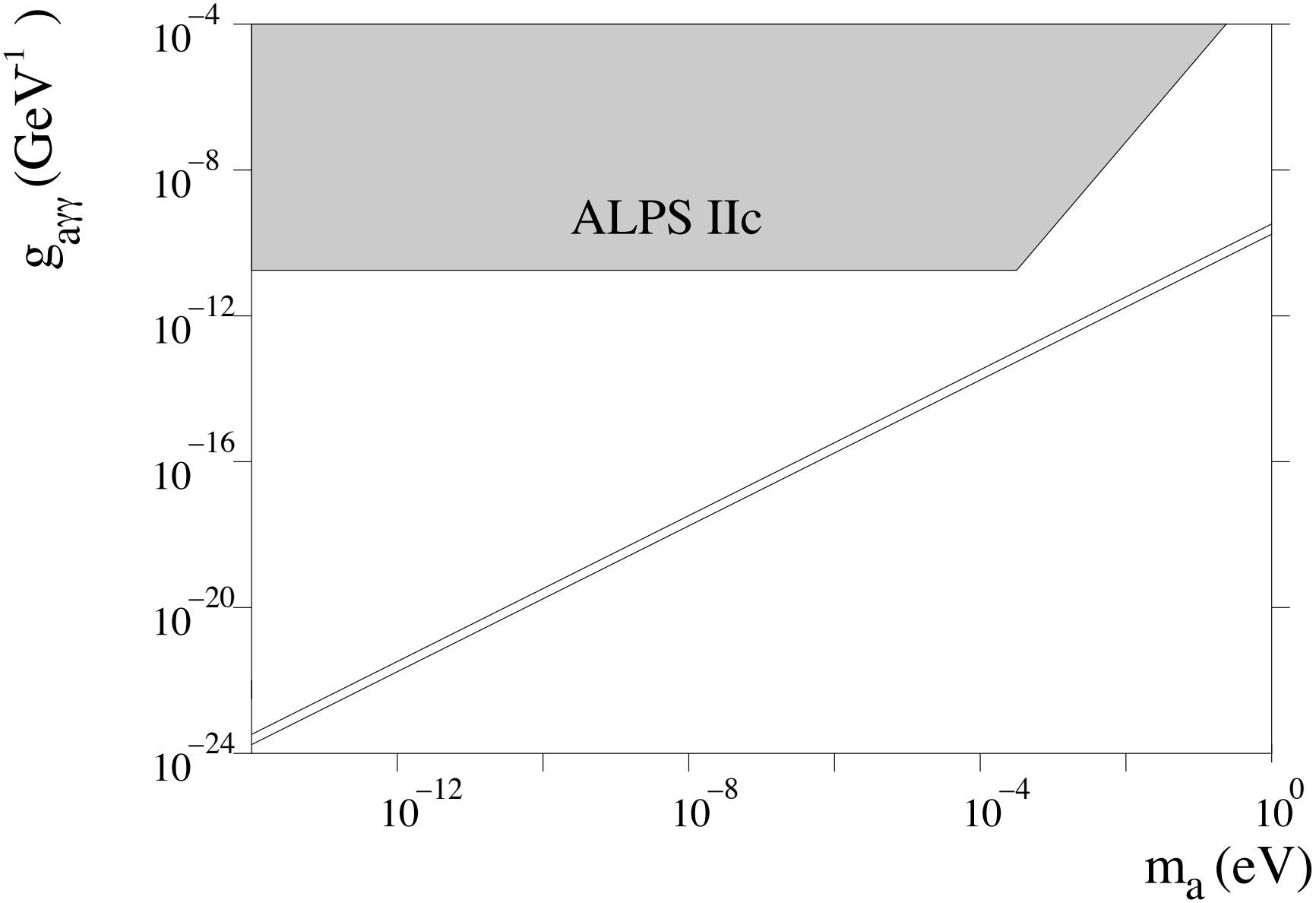
ALPS IIc
$g_{a\gamma\gamma}$ (GeV^{-1})
10^{-4}
10^{-8}
10^{-12}
10^{-16}
10^{-20}
10^{-24}
10^{-12}
10^{-8}
10^{-4}
10^{0}
m_a (eV)

Axion to magnon conversion

R. Barbieri, M. Cerdonio, G. Fiorentini and S. Vitale
Phys. Lett. B226 (1989) 357.

$$H_{a\bar{e}e} = \frac{g_e}{2f_a}\vec{\sigma}_e \cdot \vec{\nabla} a$$

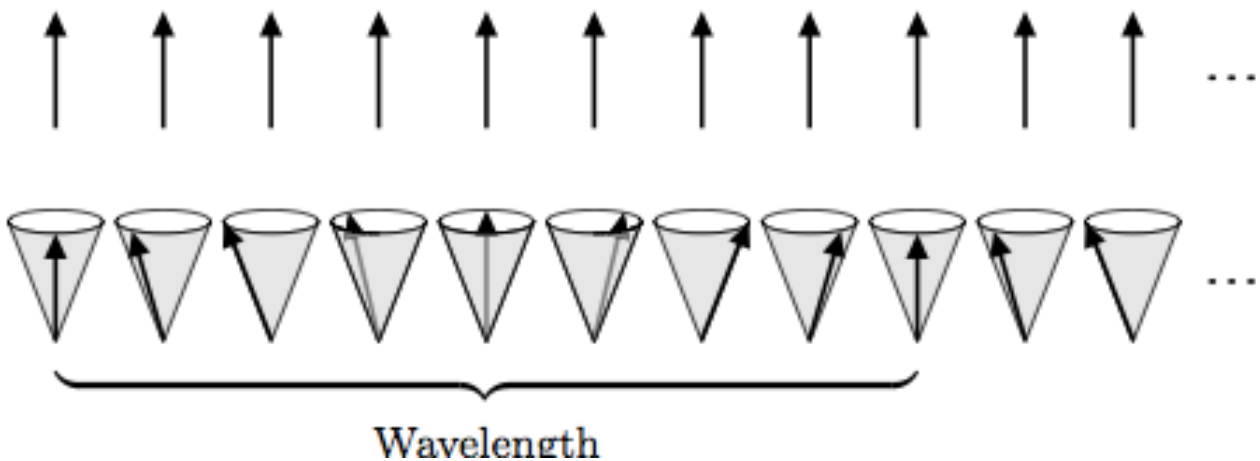

QUAX Proposal

R. Barbieri, C. Braggio, G. Carugno, C.S. Gallo, A. Lombardi, A. Ortolan, R. Pengo, G. Ruoso and C.C. Speake, arXiv: 1606.02201

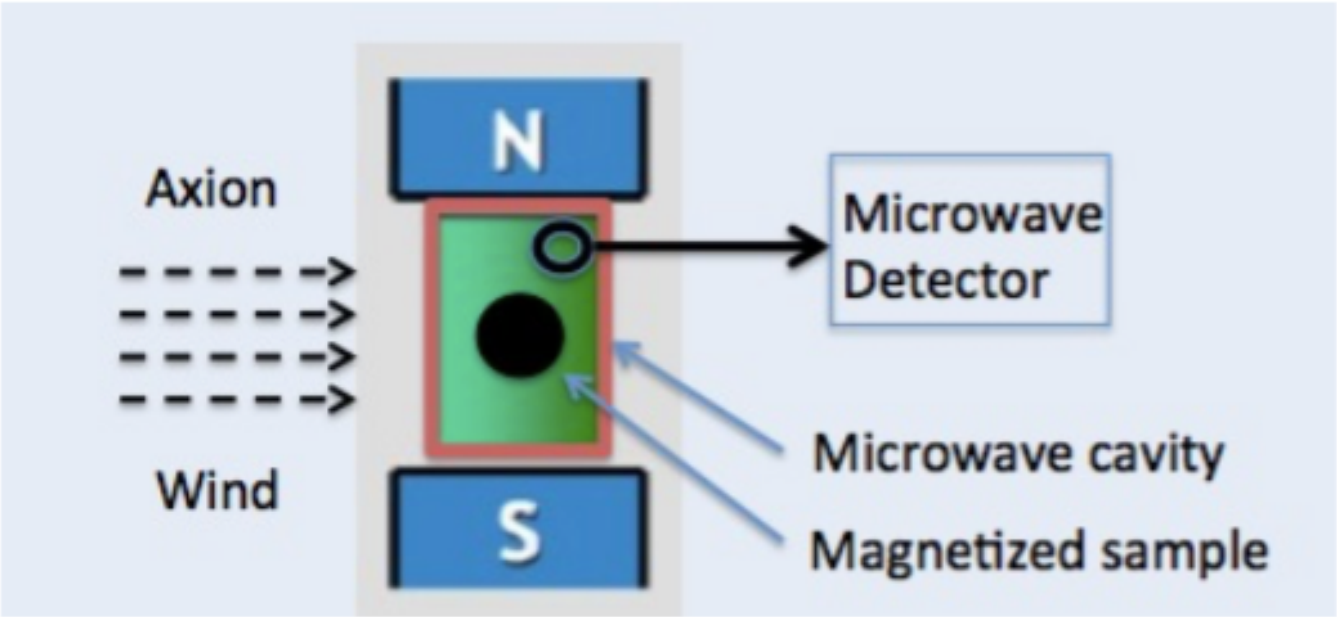

$$\text{Rate} = 1.2 \times 10^{-3} \left(\frac{m_a}{200\ \mu\text{eV}}\right)^2 \left(\frac{V}{100\ \text{cm}^3}\right) \left(\frac{n_S}{2 \cdot 10^{28}/\text{m}^3}\right) \left(\frac{\tau}{2\ \mu\text{s}}\right)$$

48 GHz

$T = 116\ mK$

NMR techniques

P. Graham, S. Rajendran; D. Budker, M. Ledbetter, A. Sushkov

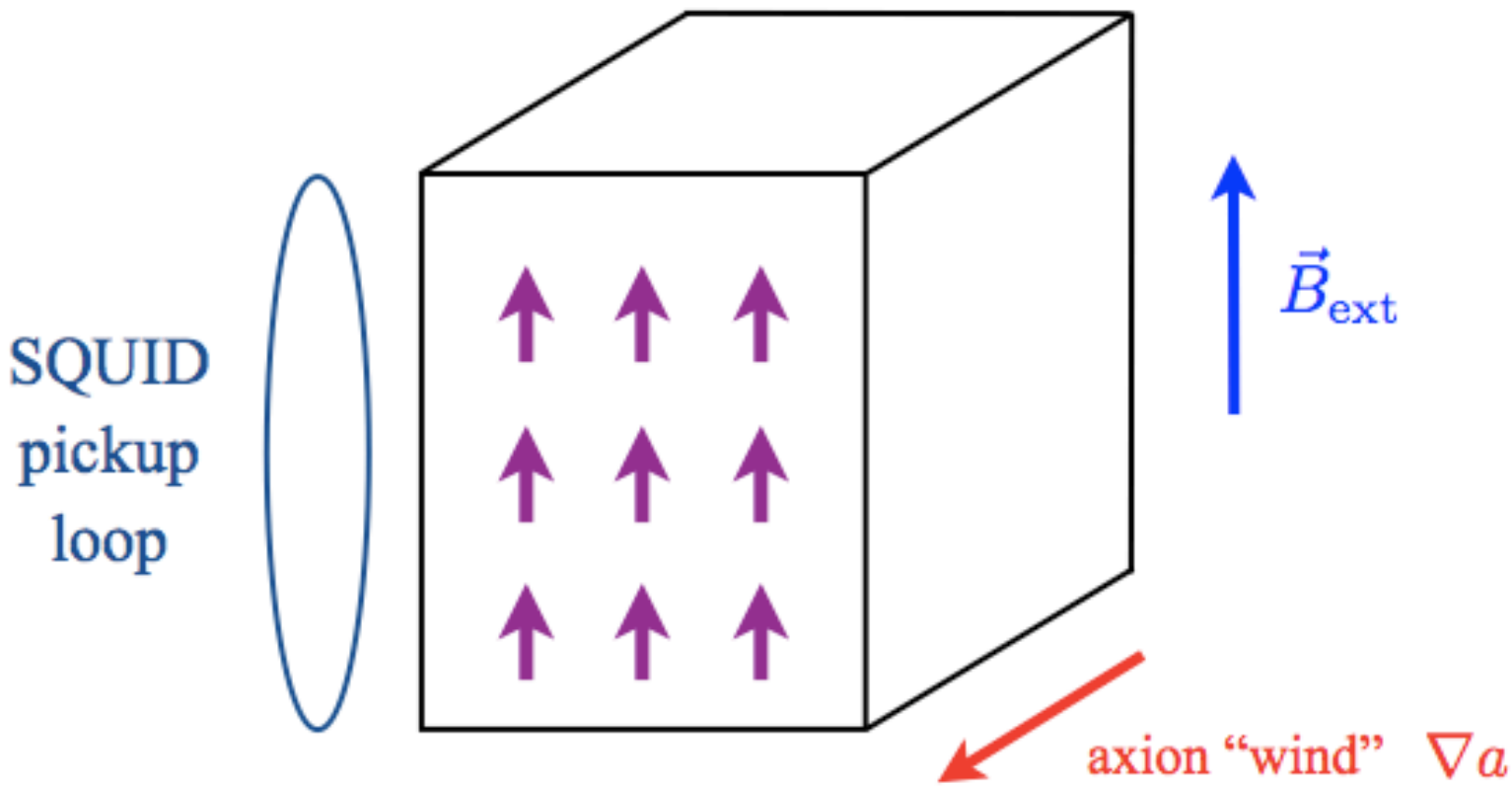

use nuclear spins coupled to axion DM

$$g_{\rm aNN}\,(\partial_\mu a)\,\bar{N}\gamma^\mu\gamma_5 N \implies H_N \supset g_{\rm aNN}\vec{\nabla}a.\vec{S}_N$$

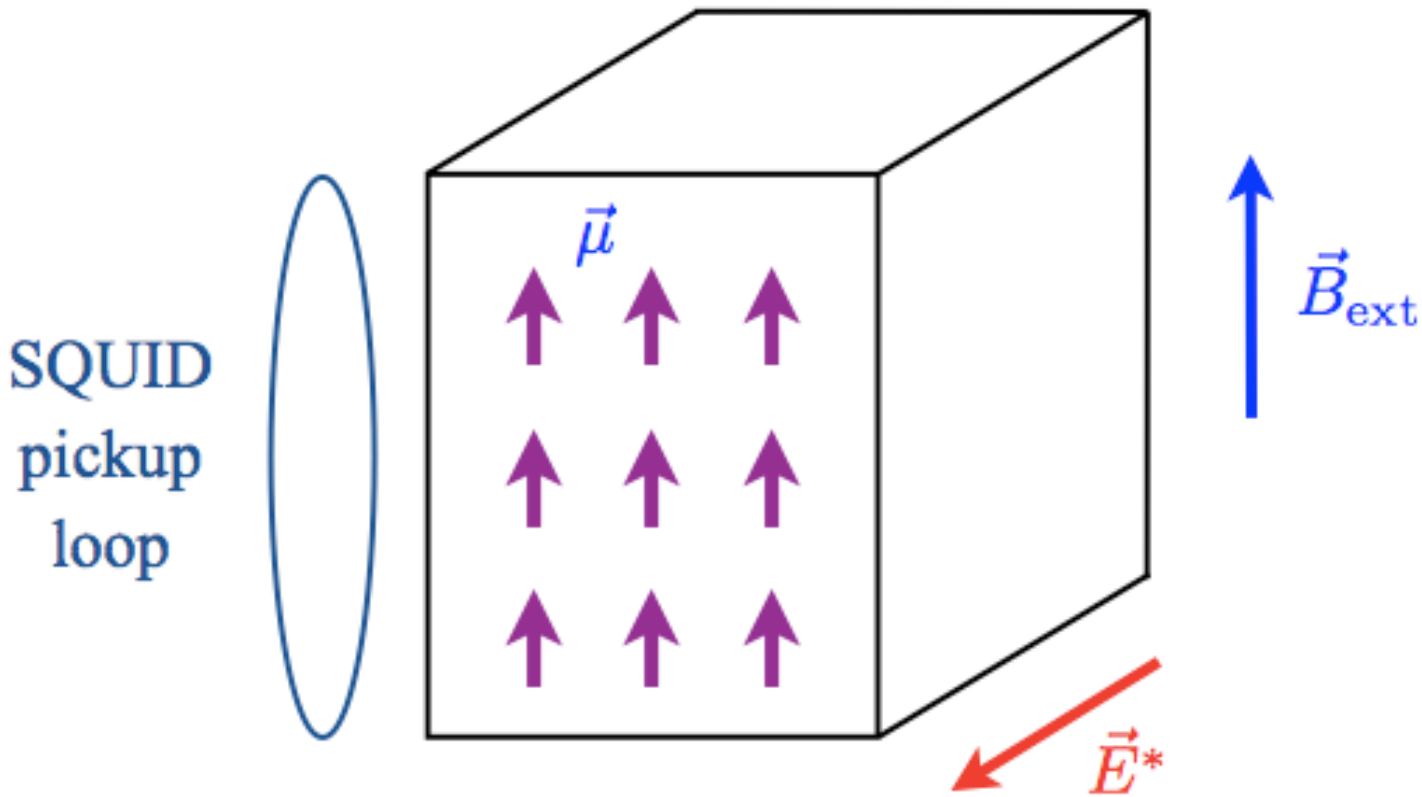

the axion field induces an oscillating nuclear electric dipole moment

$$d_e \sim 10^{-16}\ e\ \mathrm{cm}\ \frac{a(x)}{f_a}$$

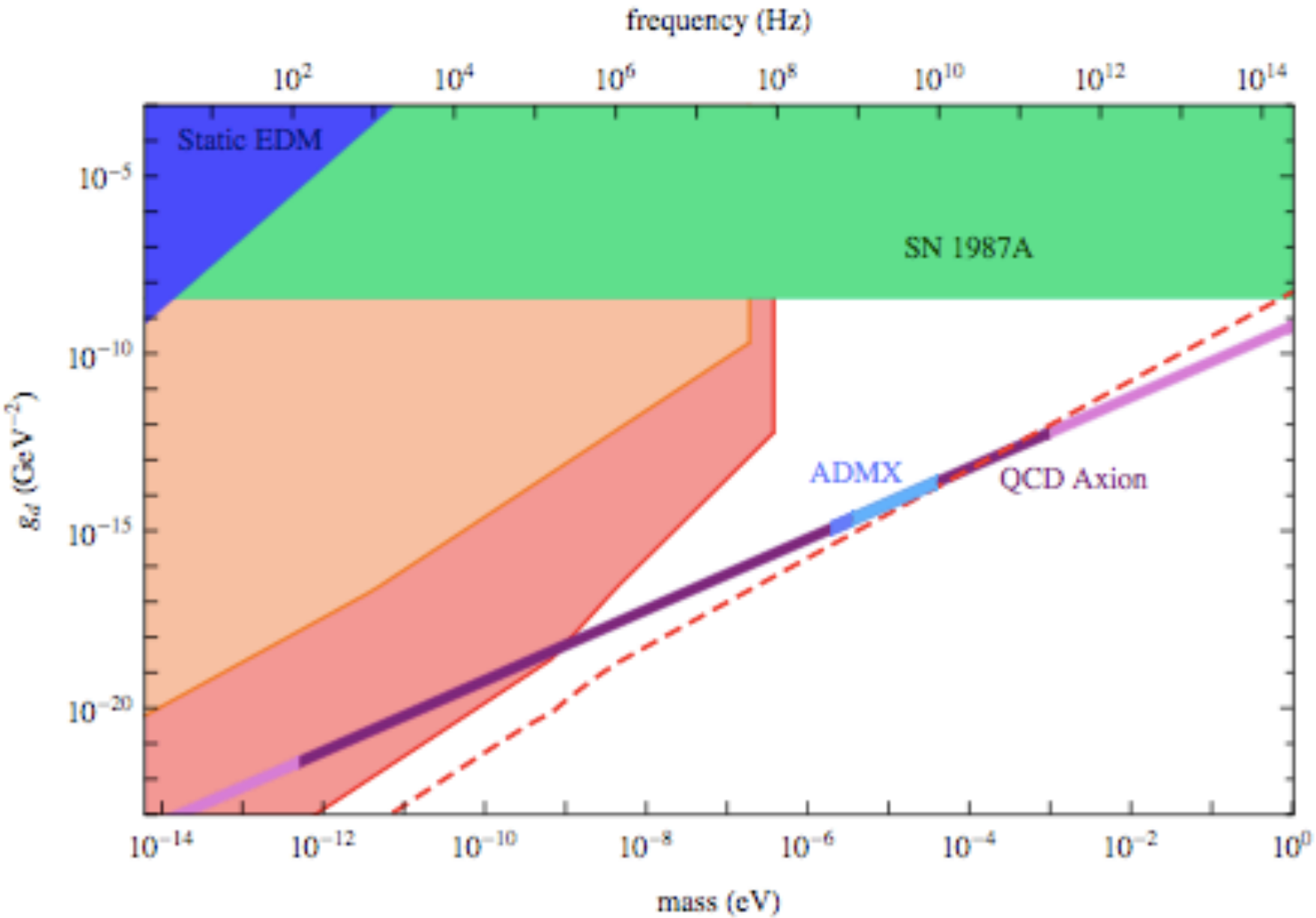

FIG. 2: Estimated constraints in the ALP parameter space in the EDM coupling g_d (where the nucleon EDM is $d_n = g_d a$ and a is the local value of the ALP field) vs. the ALP mass [17]. The green region is excluded by the constraints on excess cooling of supernova 1987A [17]. The blue region is excluded by existing, static nuclear EDM searches [17]. The QCD axion is in the purple region, whose width shows the theoretical uncertainty [17]. The solid red and orange regions show sensitivity estimates for our phase 1 and 2 proposals, set by magnetometer noise. The red dashed line shows the limit from magnetization noise of the sample for phase 2. The ADMX region shows what region of the QCD axion has been covered (darker blue) [34] or will be covered (lighter blue) [59, 60]. Phase 1 is a modification of current solid state static EDM techniques that is optimized to search for a time varying signal and can immediately begin probing the allowed region of ALP dark matter. To calculate limits from previous (static) EDM searches as well as our sensitivity curves, we assume the ALP is all of the dark matter.

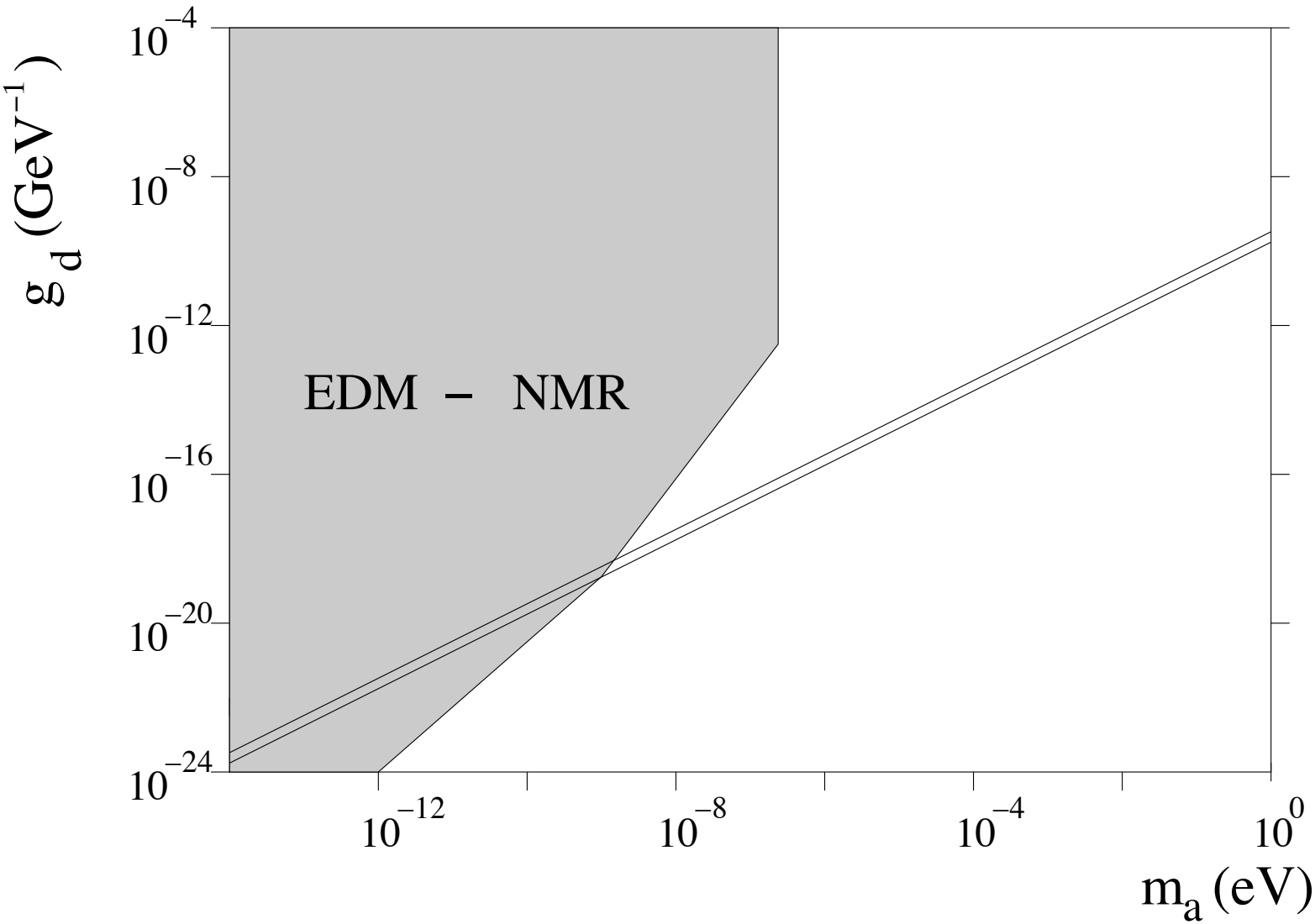
EDM − NMR
g_d (GeV^{-1})
10^{-4}
10^{-8}
10^{-12}
10^{-16}
10^{-20}
10^{-24}
10^{-12}
10^{-8}
10^{-4}
10^{0}
m_a (eV)

Axion dark matter detection using an LC circuit

PS, D. Tanner and N. Sullivan, 2013

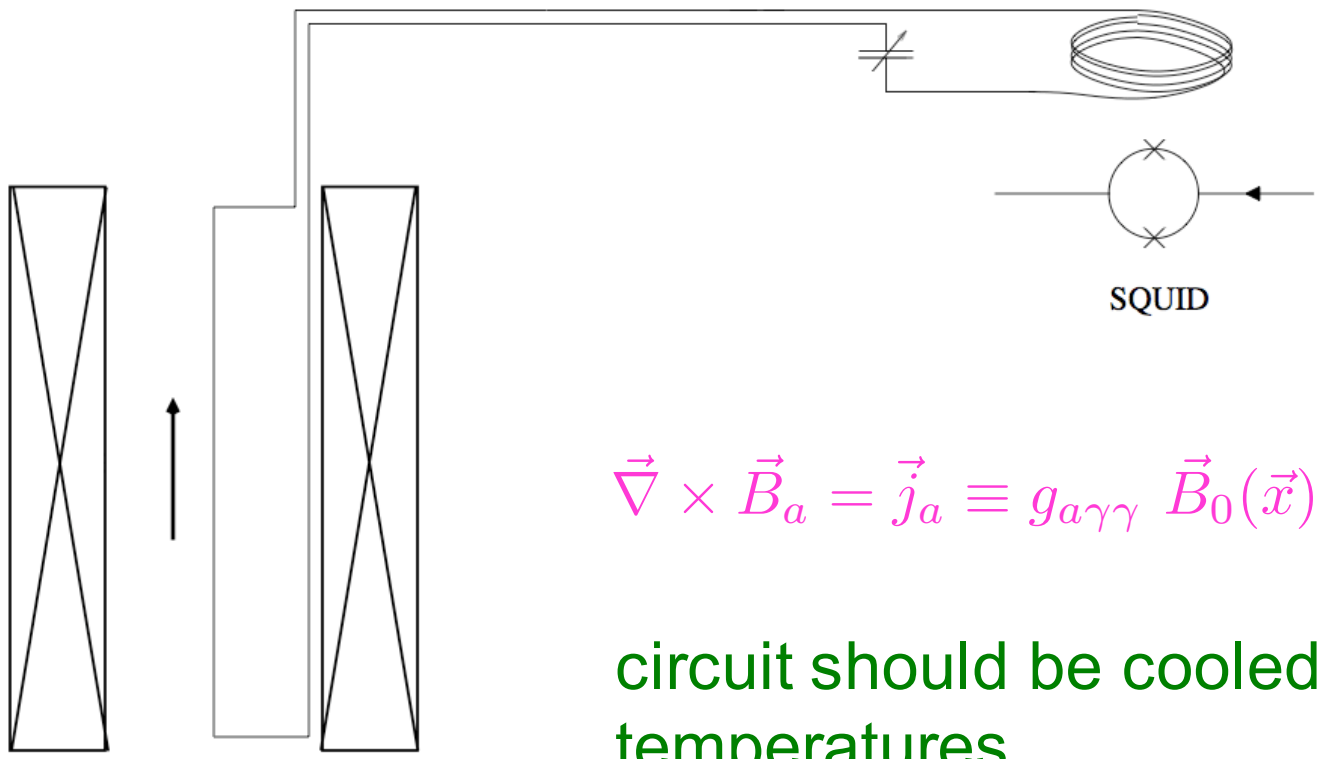

$$\vec{\nabla} \times \vec{B}_a = \vec{j}_a \equiv g_{a\gamma\gamma}\ \vec{B}_0(\vec{x})\ \partial_t a(\vec{x}, t)$$

circuit should be cooled to milli-Kelvin temperatures

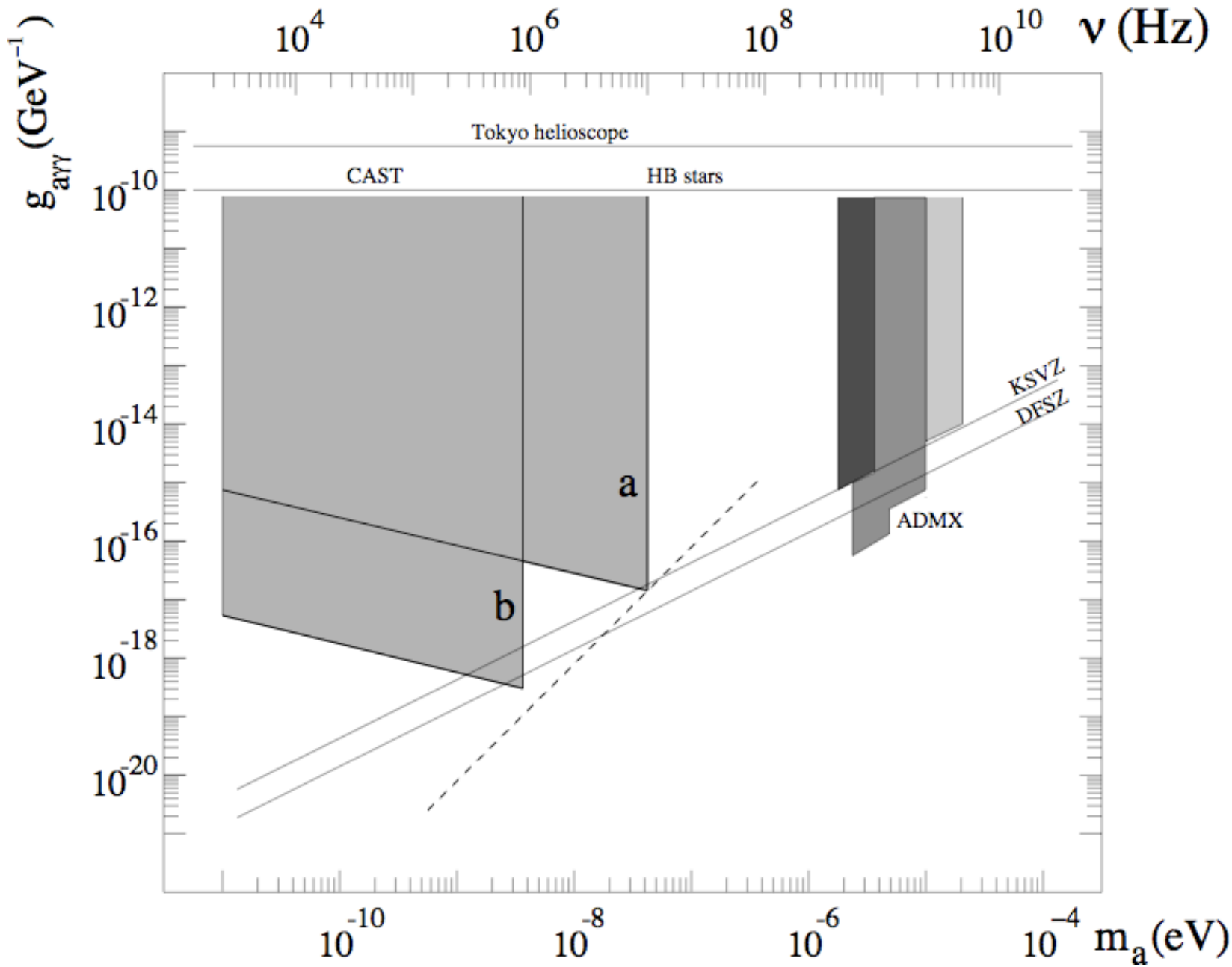

a) using ADMX magnet b) CMS magnet

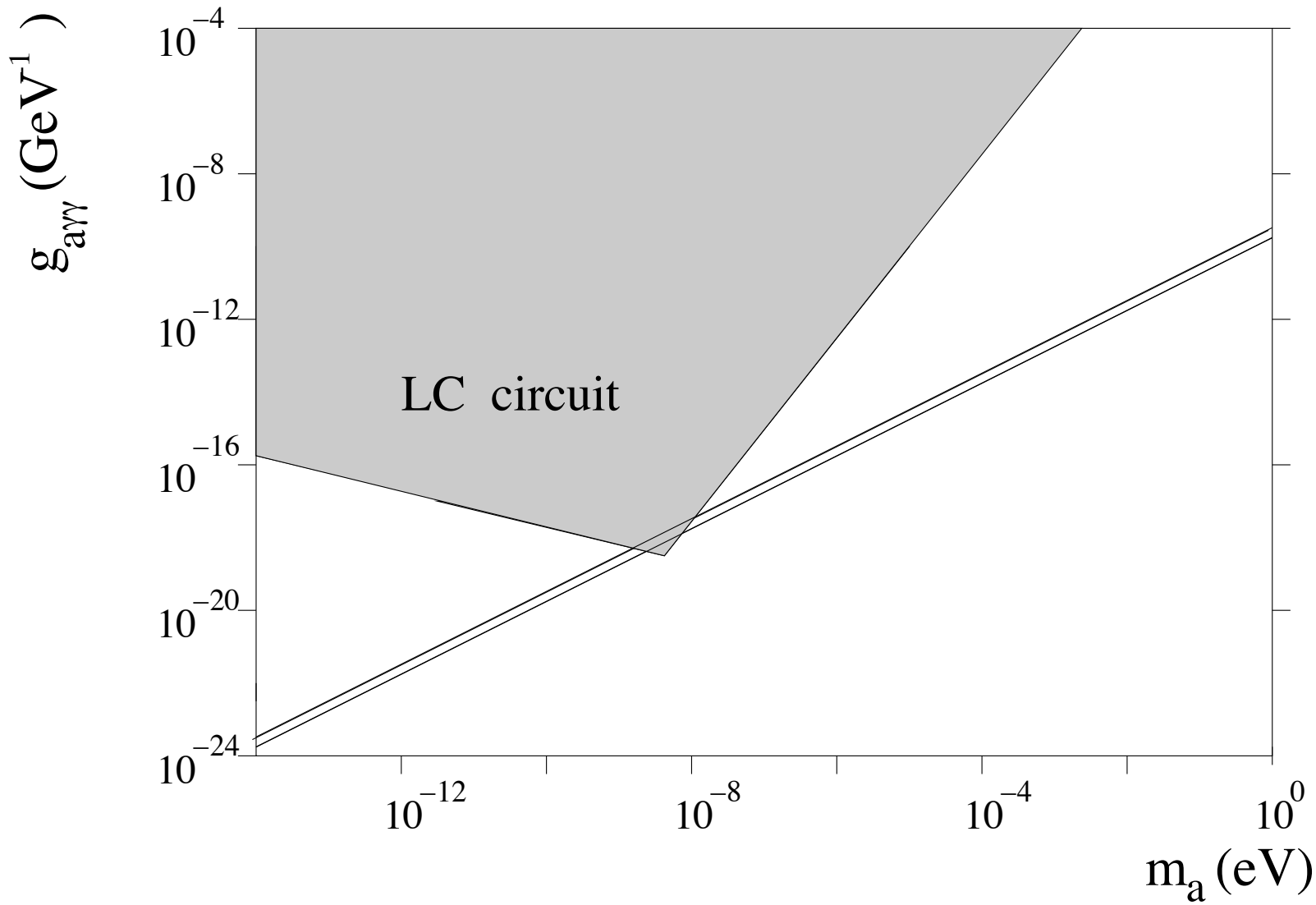
$g_{a\gamma\gamma}$ (GeV^{-1})
10^{-4}
10^{-8}
10^{-12}
10^{-16}
10^{-20}
10^{-24}
LC circuit
10^{-12}
10^{-8}
10^{-4}
10^{0}
m_a (eV)

Axion dark matter detection using atomic transitions

PS 2014

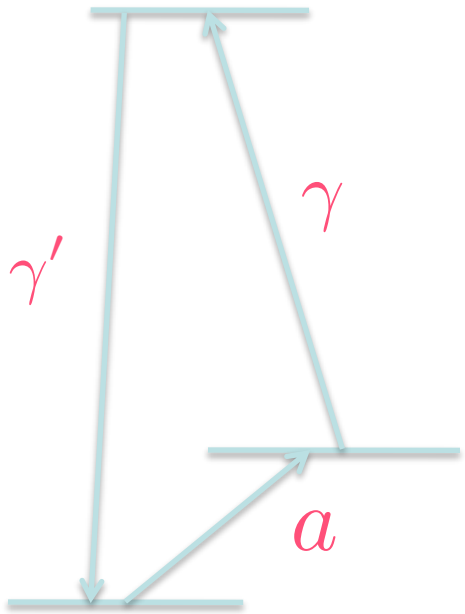

$$\mathcal{L}_{a\bar{f}f} = -\frac{g_f}{2f_a}\partial_\mu a(x)\bar{f}(x)\gamma^\mu\gamma_5 f(x)$$

$$f \text{ is electron, or nucleon}$$

$$H_{a\bar{f}f} = +\frac{g_f}{2f_a}\vec{\sigma}_f \cdot \vec{\nabla} a$$

- tune using the Zeeman effect
- use laser techniques to count axion induced transitions
- must cool to milli-Kelvin temperatures

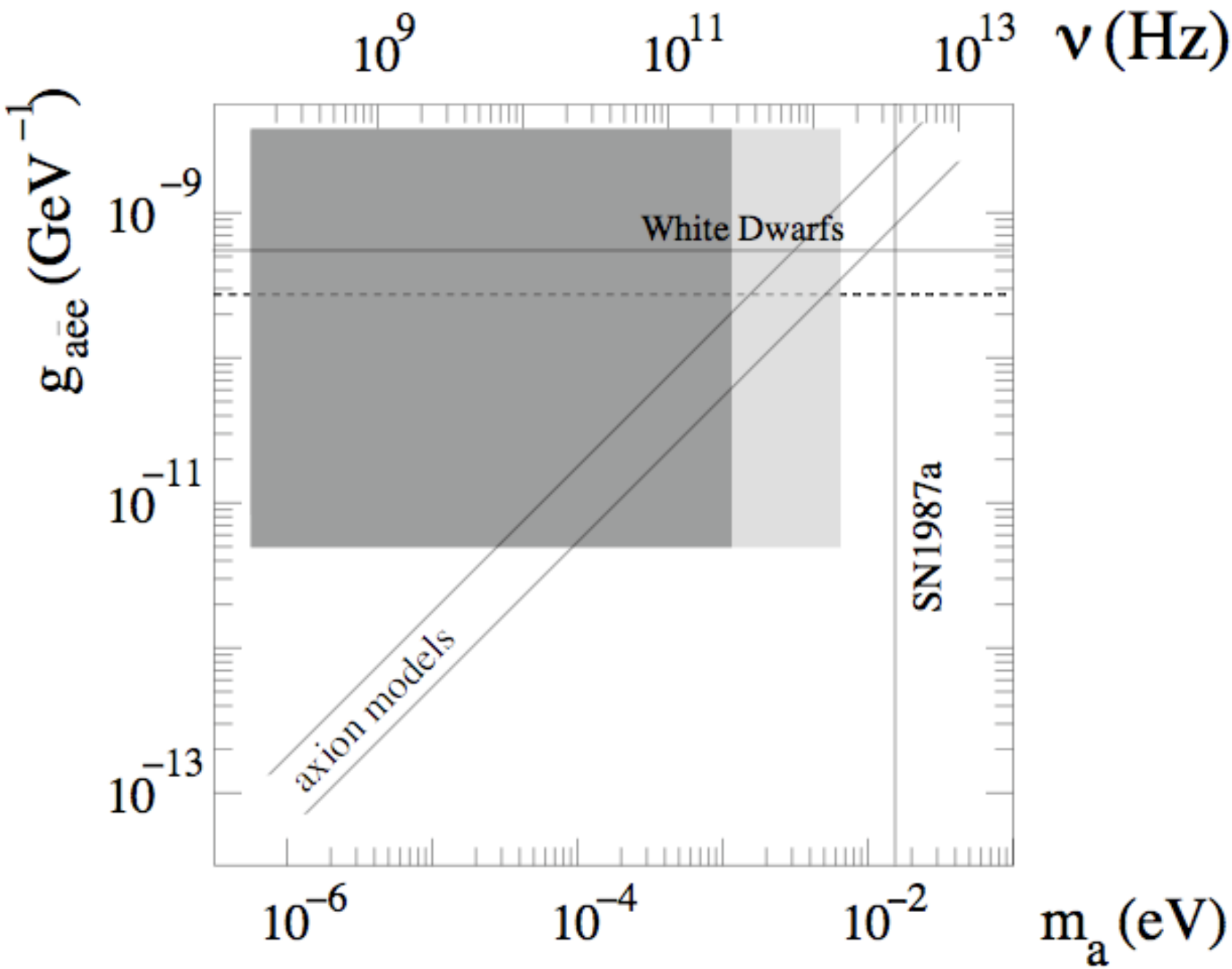
10^9
10^{11}
10^{13}
ν (Hz)
$g_{a\bar{e}e}$ (GeV^{-1})
10^{-9}
10^{-11}
10^{-13}
White Dwarfs
axion models
SN1987a
10^{-6}
10^{-4}
10^{-2}
m_a (eV)

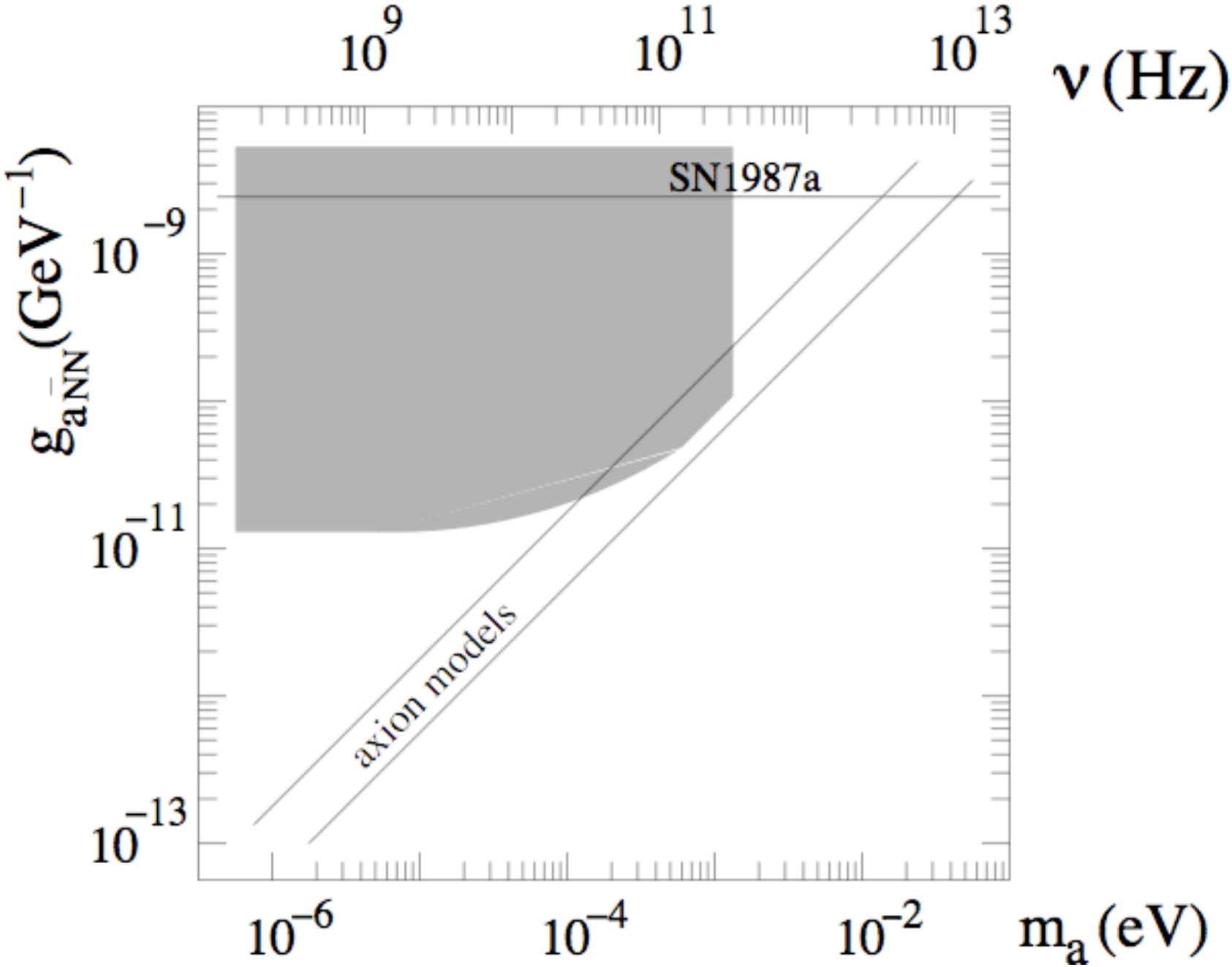
10^{9}
10^{11}
10^{13}
ν (Hz)
SN1987a
$g_{a\bar{N}N}$ (GeV^{-1})
10^{-9}
10^{-11}
10^{-13}
axion models
10^{-6}
10^{-4}
10^{-2}
m_a (eV)

Wire array detector

PS, D. Tanner and Y. Wang, 1992

G. Rybka, A. Wagner et al. 2004

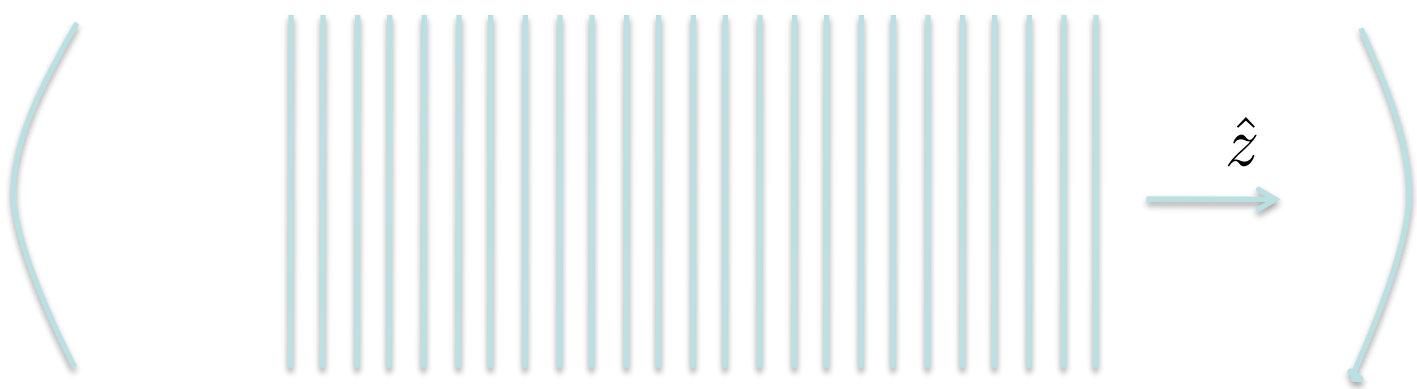

- pass currents through superconducting wires
- produce $\vec{B} = \hat{x} B_0 cos(qz)$
- enhance the quality factor by placing the array in a confocal resonator
- tune to $q = m_a$

Dielectric Haloscope

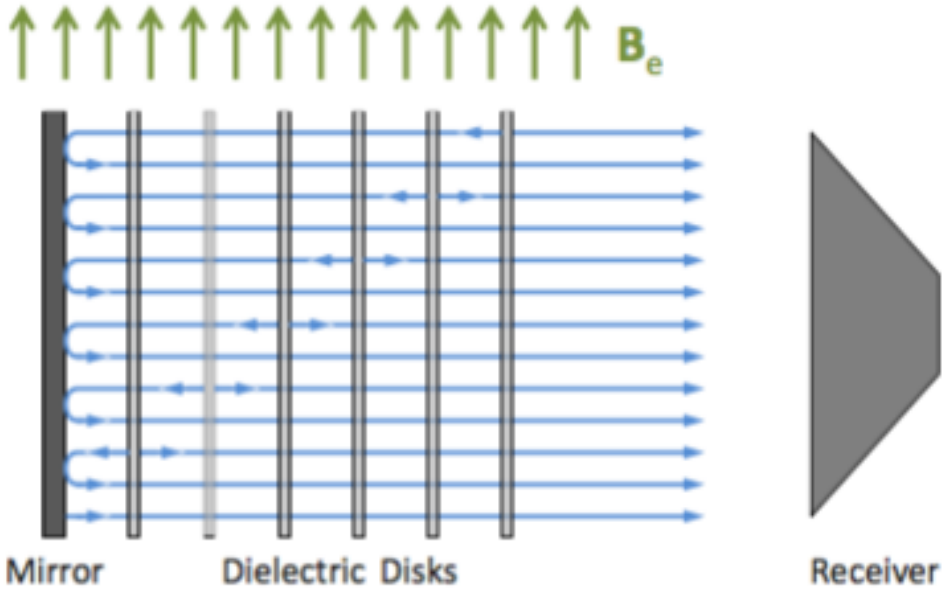

FIG. 1. A dielectric haloscope consisting of a mirror and several dielectric disks placed in an external magnetic field $\mathbf{B}_e$ and a receiver in the field-free region. A parabolic mirror (not shown) could be used to concentrate the emitted power into the receiver. Internal reflections are not shown.

A. Caldwell et al., arXiv 1611.05865 (Madmax)

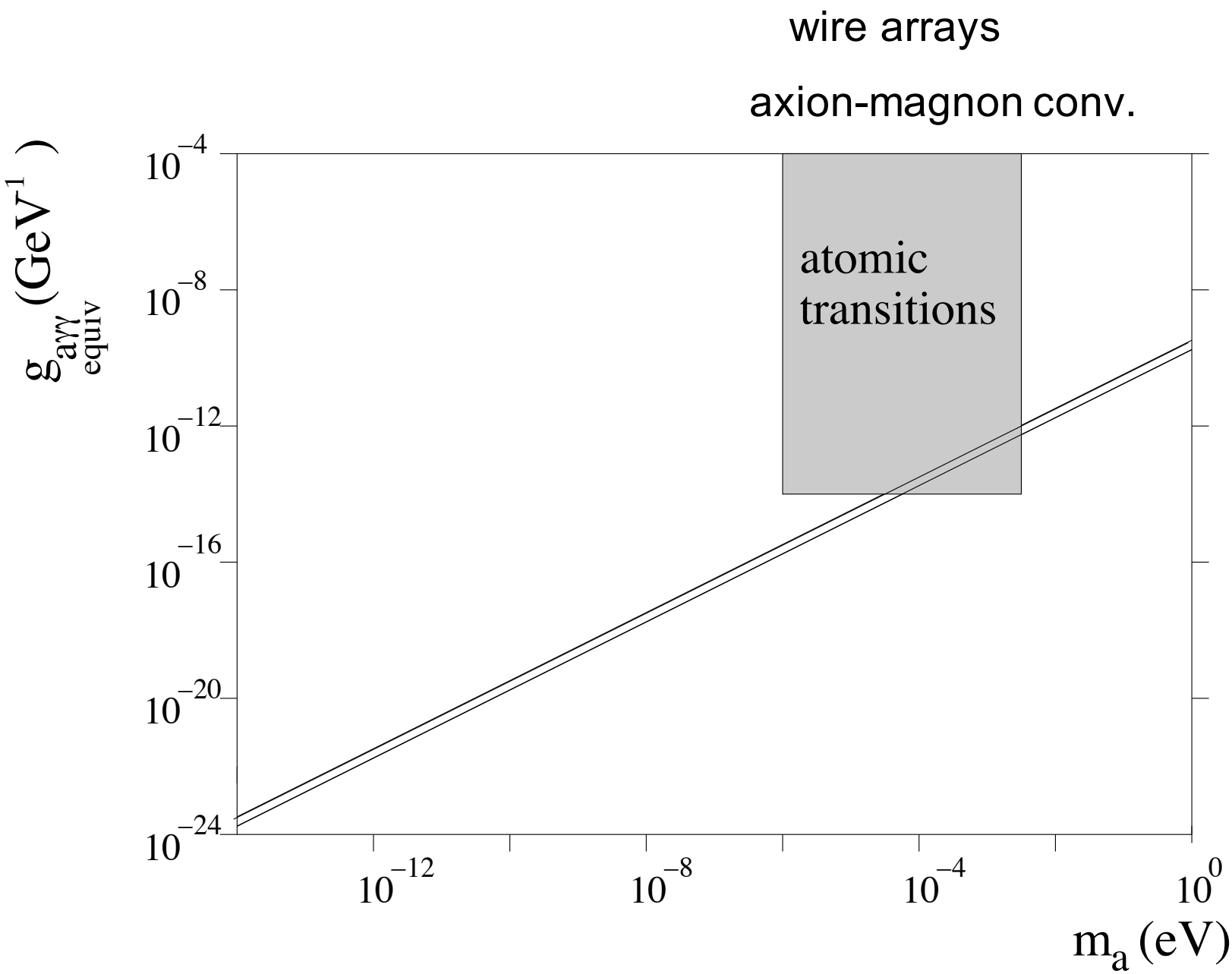
wire arrays
axion-magnon conv.
atomic
transitions
$g_{a\gamma\gamma}$ (GeV^{1})
equiv
10^{-4}
10^{-8}
10^{-12}
10^{-16}
10^{-20}
10^{-24}
10^{-12}
10^{-8}
10^{-4}
10^{0}
m_a (eV)

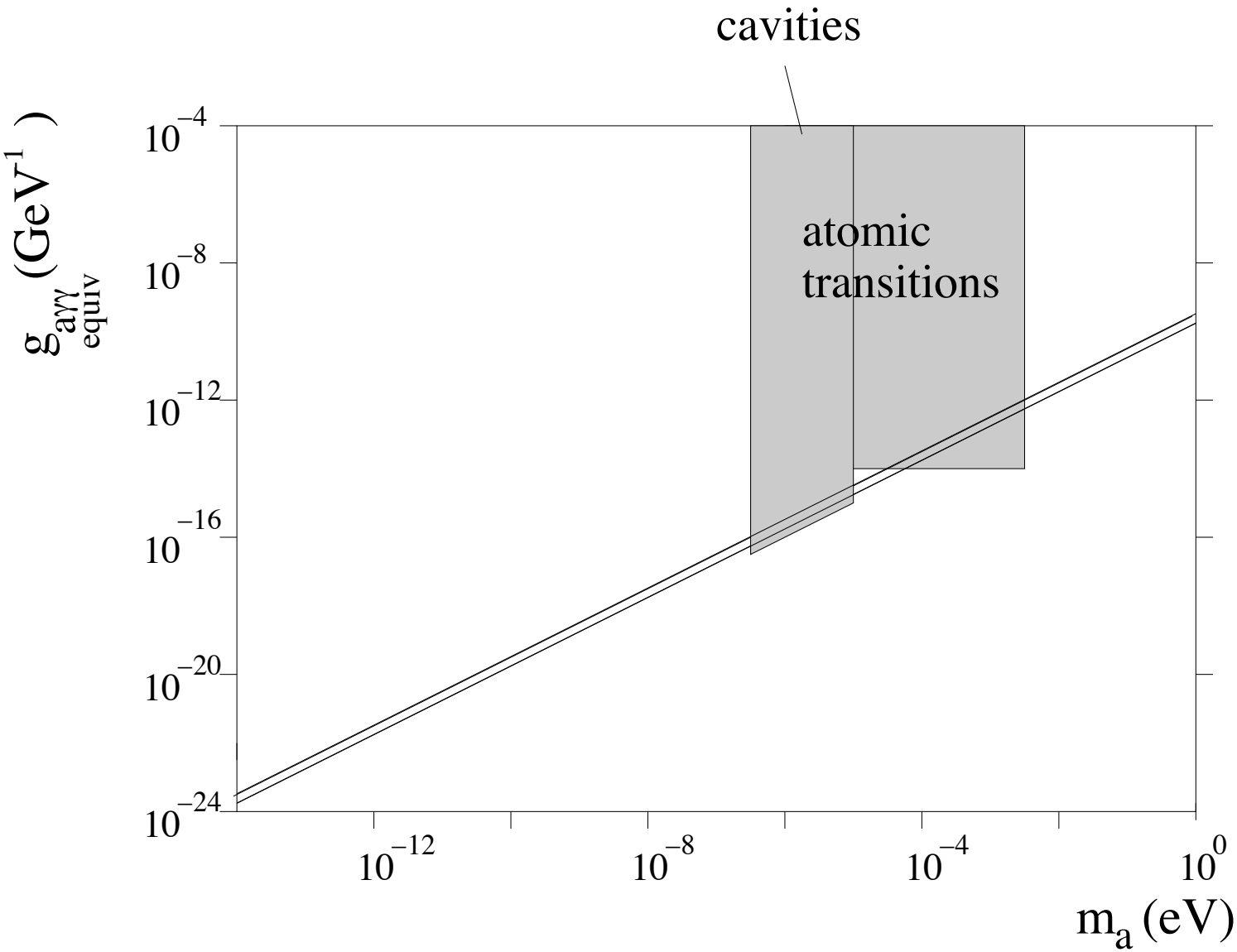
cavities
atomic
transitions
$g_{a\gamma\gamma\,\mathrm{equiv}}$ (GeV^{-1})
10^{-4}
10^{-8}
10^{-12}
10^{-16}
10^{-20}
10^{-24}
10^{-12}
10^{-8}
10^{-4}
10^{0}
m_a (eV)

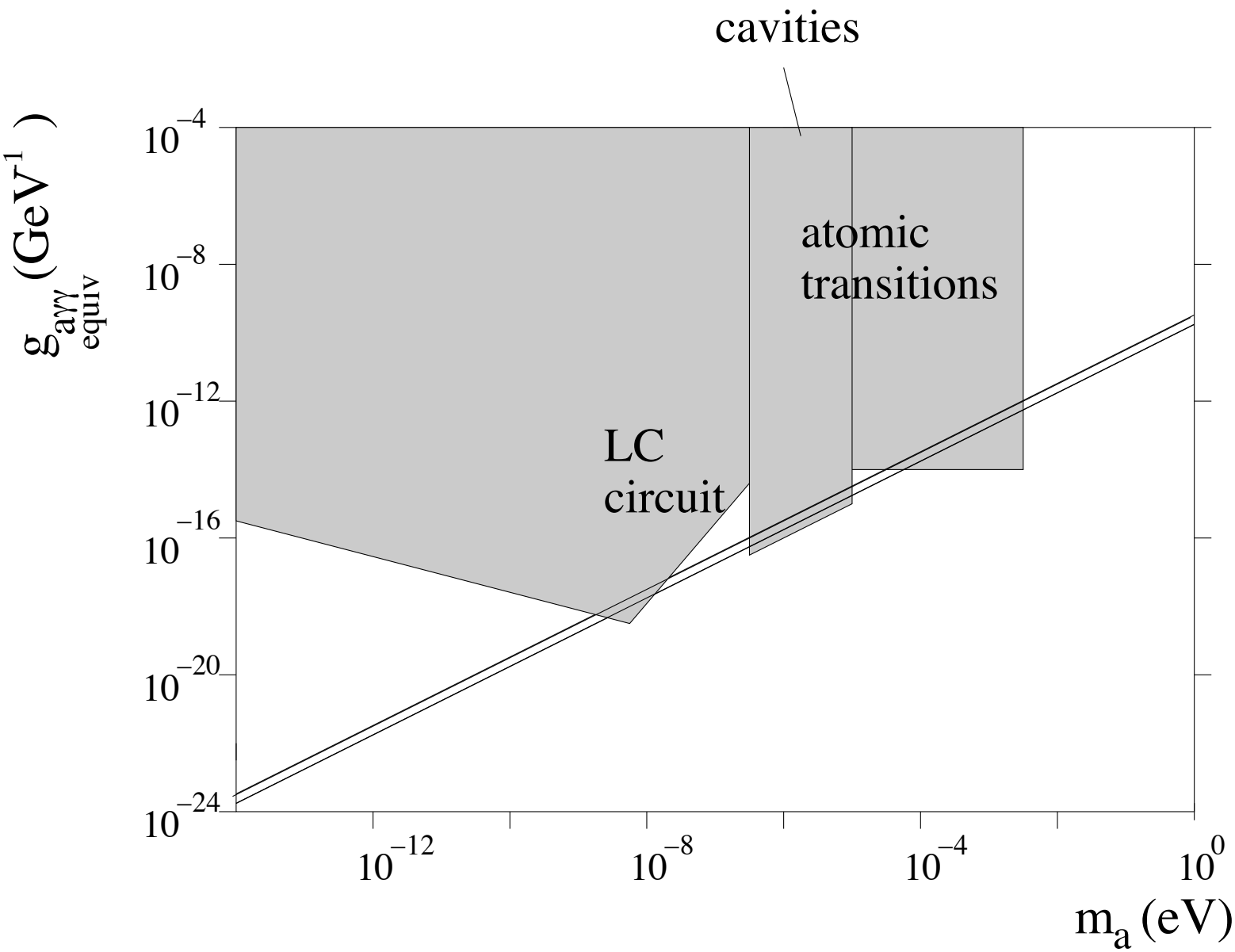
cavities
atomic
transitions
LC
circuit
$g_{a\gamma\gamma_{equiv}}$ (GeV^{-1})
10^{-4}
10^{-8}
10^{-12}
10^{-16}
10^{-20}
10^{-24}
10^{-12}
10^{-8}
10^{-4}
10^{0}
m_a (eV)

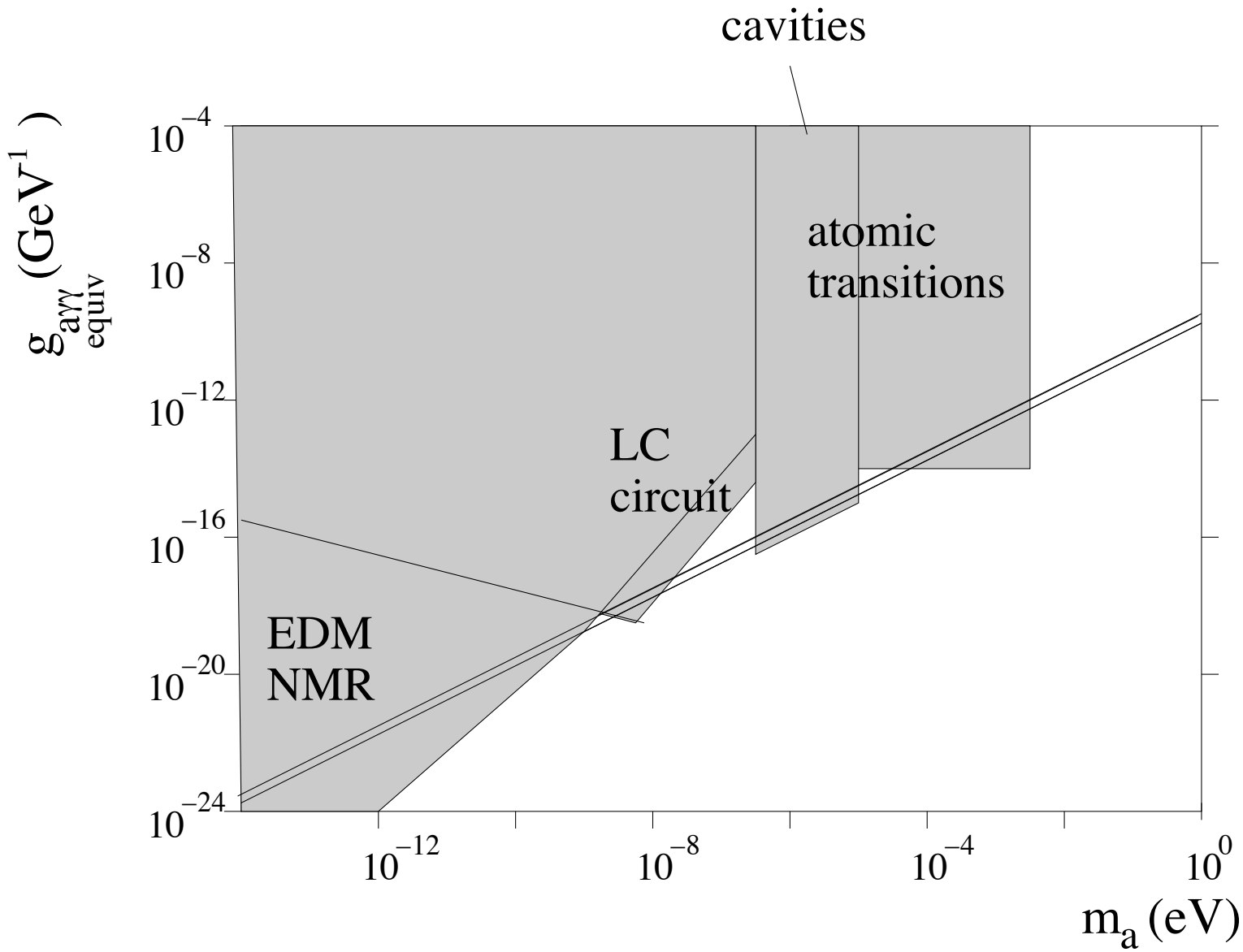
cavities
atomic
transitions
LC
circuit
EDM
NMR
$g_{a\gamma\gamma\,\mathrm{equiv}}$ (GeV^{-1})
10^{-4}
10^{-8}
10^{-12}
10^{-16}
10^{-20}
10^{-24}
10^{-12}
10^{-8}
10^{-4}
10^{0}
m_a (eV)

Conclusions

- Axion dark matter is well motivated
- Axion dark matter can be detected over most of the plausible mass range

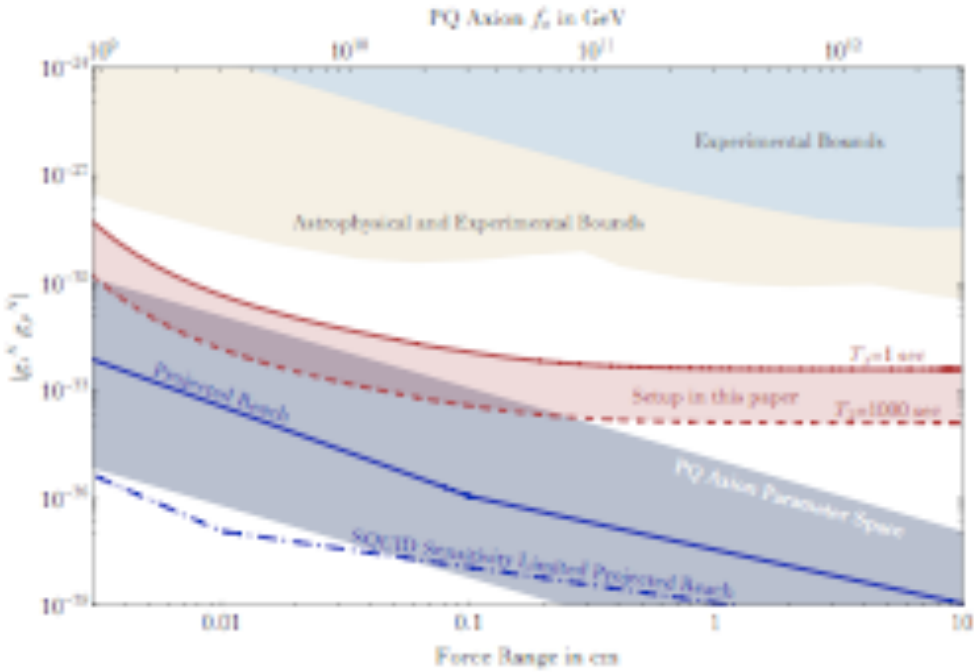

FIG. 2: Reach in the coupling vs interaction range plane for the monopole-dipole axion mediated interactions. The band bounded by the red (dark) solid line and dashed line denotes the limit set by transverse magnetization noise of the sample for the specific setup described in the text, for T_2 ranging from 1 s to 1000 s. The blue (darker) solid line is a future projection obtained by scaling the setup using parameters chosen in Table 1. The blue (darker) dot-dashed line is the projected limit set by the SQUID sensitivity. We limit the integration time in all setups to 10^6 sec. The shaded band is the parameter space for the PQ axion with $C_f = 1$. Additional uncertainties [14] and model dependence [15] can produce variations of this axion parameter space. Experimental as well as combined experimental and astrophysical bounds are also presented [9, 11].